Synthesis and Characterization of Iron-doped TiO_2 Immobilized on to Cellulosic Nanocomposite for the removal of Organic Contaminants

A
Dissertation Report
Submitted in Partial Fulfilment of the Requirement
For the Award of the Degree of

Master of Science
in
Biotechnology

Komal Jindal
Registration no. 301701016

Under the Supervision of:
Dr. Shekhar Agnihotri

THAPAR INSTITUTE
OF ENGINEERING & TECHNOLOGY
(Deemed to be University)

Department of Biotechnology
TIET, Patiala
July 2019

CERTIFICATE

This is to certify that dissertation project entitled **"Synthesis and Characterization of Iron- doped TiO_2 Immobilized on to Cellulosic Nanocomposite for the removal of Organic Contaminants"** submitted by **Ms. Komal Jindal** (Roll No. 301701016) in the partial fulfillment for the award of degree of **Master of Science** in Biotechnology from Thapar Institute of Engineering & Technology, Patiala, Punjab, is the record of the candidates' own independent and original research work carried out under my supervision and guidance. The matter embodied in this dissertation has not been submitted in part to any other University/Institute for the award of any degree or diploma in India.

Dr. Shekhar Agnihotri
Supervisor
Assistant Professor
Department of Biotechnology
TIET, Patiala-147001

Prof. Moushumi Ghosh
Head
Department of Biotechnology
TIET, Patiala-147001

DECLARATION

I hereby declare that the work which is being presented in dissertation entitled entitled **"Synthesis and Characterization of Iron- doped TiO_2 Immobilized on to Cellulosic Nanocomposite for the removal of Organic Contaminants"** submitted by me for the award of the degree of **Master of Science** in Department of Biotechnology, TIET University, Patiala is true and original record of my own independent and original research work carried out under the supervision of Dr. Shekhar Agnihotri. Further, I declare that no part of this dissertation has been submitted to any other University/Institute for the award of any degree in India or abroad.

Place: Patiala

Date: 9/8/2019

Komal Jindal

Komal Jindal

ACKNOWLEDGEMENT

I have taken efforts in this project. However, it would not have been possible without the kind support and help of many individuals and organization. I would like to extend my sincere thanks to all of them. I am highly obligated to my guide **Dr. Shekhar Agnihotri** for his guidance and constant supervision as well as for providing necessary information regarding the project & also for their support in completing the project.

I express my deep sense of gratitude to **Prof. Moushami Ghosh**, (Head, Department of Biotechnology) and **Dr. Anil Kumar** (Head, TIFAC-CORE) for providing me the opportunity and all necessary facilities during the tenure of my work.

I would like to express my gratitude towards all the research scholars **Ms. Anjali Chauhan, Mr. Devendra Sillu, Ms. Navneet Kaur** for their kind co-operation and encouragement which help me in the completion of this project. I would also like to express my special thanks to my lab mates **Ms. Anushka Garg, Ms. Shubhangi Jain and Mr. Yeshaswi Kaushik** for giving me thoughtful advices and motivation to do my work with precision.

A special thanks to **Dr. Bonamali Pal** and **Dr. Soumen Basu** for providing the access to BET and DLS. I thank their research scholars **Ms. Smriti Thakur** and **Ms. Surbhi Sharma** for their assistance and valuable time.

I also acknowledge the funding from **DST-SERB (YSS/ES/001599, dates 22.03.2016) and TIET Seed Grant (TIET/DORSP/57/474, dated 26.03.2017)** for executing their research work.

I would like to mention the unconditional support from my family, whose blessings boosted me to achieve my destination. My loving thanks to my father, **Mr. Sushil Kumar;** my mother, **Mrs. Krishna;** my younger sister **Ms. Mehak Jindal,** and my younger brother **Mr. Krish Kumar.**

Place: Patiala

Komal Jindal

Date: 9/8/2019

Komal Jindal

TABLE OF CONTENTS

LIST OF FIGURES

LIST OF TABLES

LIST OF ABBREVIATIONS & SYMBOLS

ABBREVIATIONS	FULL FORMS
TiO_2	Titanium dioxide
Fe	Iron
ZnO	Zinc oxide
eV	electron Volt
e^-	Electrons
h^+	Holes
mg	Milligram
nm	Nanometre
AOPs	Advanced Oxidation Processes
NPs	Nanoparticles
Ag	Silver
C	Carbon
N	Nitrogen
Cu	Copper
Au	Gold
Pt	Platinum
CB	Conduction band
VB	Valance band
MB	Methylene Blue
DRS	Diffuse Reflectance Spectroscopy
DLS	Dynamic Light Scattering
XRD	X-Ray Diffraction
BET	Brunaer-Emmett-Teller
FT-IR	Fourier transform-Infrared Spectroscopy
SEM	Scanning Electron Microscope
EDX	Energy Dispersive X-Ray Spectroscopy
Rpm	rotation per minute
Ppm	parts per million
OD	optical density
$OH^{\bullet}$	Hydroxyl radicals
ng	nano gram
mg	milligram
%	percentage

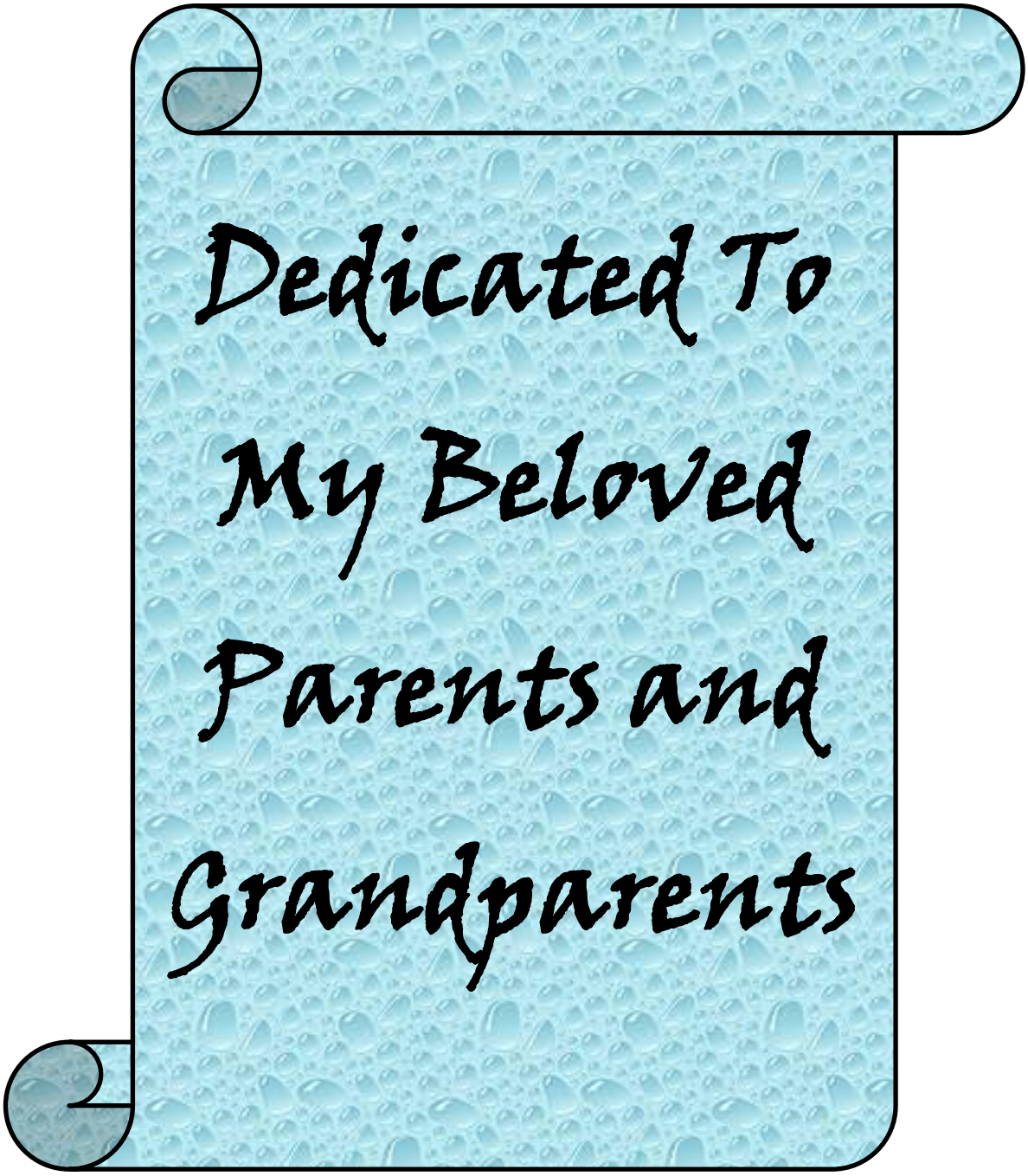
Dedicated To
My Beloved
Parents and
Grandparents

ABSTRACT

In the processing of textile dyes and pharmaceutical compounds, large amount of waste is generated which directly or indirectly gets disposed-off into water streams. This has led to the undesirable toxicity of surface as well as ground water inducing negative impact on organisms residing in aquatic water bodies and humans. Therefore, it becomes necessary to efficiently remove these organic compounds from municipal as well as industrial effluents. In view of the aforementioned requirement heterogeneous photocatalysis act as cost-effective approach in lieu of conventional wastewater treatment technologies. In present study, TiO_2 (Titanium dioxide) nanoparticles were synthesized chemically using solution route. As TiO_2 is active only under Ultraviolet (UV) exposure, doping with iron (Fe) is performed to alter its surface properties and make it visible light responsive. To further improve its separation and reusability the doped TiO_2 is mixed with biodegradable support matrix i.e. microcrystalline cellulose (MC). The synthesized bionanocomposite was characterized through Diffuse Reflectance Spectroscopy (DRS), Dynamic Light Scattering (DLS), X-Ray Diffraction Spectroscopy (XRD), Zeta Potential (ZP), Brunauer-Emmett-Teller (BET), Fourier-infrared Transform Spectroscopy (FTIR), Scanning Electron Microscopy (SEM) and Energy Dispersive X-Ray Analysis (EDX) to study their surface and morphological properties. The resulting bionanocomposite showed a significant photocatalytic degradation of methylene blue ~95% and diclofenac ~84% within 120 minutes of solar irradiation. Reusability tests were carried out in order to check the economic viability of bionanocomposite which was found to be 49% even after 8 consecutive uses. Kinetics of photocatalytic degradation was modelled against different equations in order to elucidate the trend of degradation which was found to be pseudo-first order. Thus this study suggested the use of Fe-TiO_2-cellulose as a green and sustainable catalyst for wastewater treatment without leaving any photocatalyst in the reaction system hence contributing towards use of green technology system.

Keywords: Photocatalysis, Bionanocomposite, Reactive oxygen species, Methylene blue, Diclofenac

CHAPTER 1

Introduction

The worldwide increase in population has led to improved recognition and understanding for better health and lifestyle leading to rapid industrialization. This abrupt development of industries add huge amount of recalcitrant compounds to water bodies (Agnihotri *et al*., 2018). Among different sources, industries engaged with chemical manufacturing such as dyes and pharmaceuticals produces enormous amount of pollutants which sometimes untreated or maybe partially treated are being introduced in the water streams. Dyes are complex organic molecules, which when applied to any fabric dispense color used in various industries such as paper, textile, leather tanning, plastics, food processing etc. (Yagub *et al*., 2014). This process requires lot of water adding harmful adulterants to water bodies such as acid and alkalis. In addition to dyes, pharmaceutical active compounds present in surplus amount are responsible to alter the properties of water. The major sources of pharmaceuticals in water bodies include leakages occurred at manufacturing units, excretion of drugs through urine and unused medicines disposal in domestic and hospital wastes (Moctezuma *et al*., 2012).

The global application of dyes and pharmaceuticals has resulted in negative impact on both aquatic as well as terrestrial ecosystem. About 7 X 10^5 tons of synthetic dyes are being manufactured in industries out of which 10-50% of colorants are departed to water bodies unrefined causing water pollution (Teh *et al*., 2011). Moreover with the increasing need of pharmaceuticals the global annual drug consumption ranges from 100,000-200,000 tons among nations like India, Brazil, China, South Africa and Russia holding major proportion (IBEF 2019). These contaminants when remain in contact with humans and animals for longer period affect biological balance and human health. Frequent studies have shown the feminizing effect on male fishes because of estrogen and certain chemicals behaving like that, causing alteration in ratios of females to males (Chauhan *et al*., 2019). They cause mortality, reproduction problems, immobilization and inhibition of growth in terrestrial ecosystem (Lee *et al*., 2017). The widespread existence of these compounds causes serious skin rashes, chronic respiratory infections, allergy, cancer in humans,

vomiting, nausea, acute toxicity, mutagenicity and eutrophication by blocking sunlight and oxygen in water (Agnihotri *et al*., 2018).

These beformentioned issues have raised the concern regarding possible methods for effective removal of recalcitrant compounds from wastewater. There has been a considerable amount of research in the development of sustainable water treatment technique among which the most employed one was the conventional method. These methods helps in removing organic matters, solids and sometimes nutrients by fusion of physical, chemical and biological technologies such as screening, mixing, adsorption, ion-exchange, activated sludge process, filtration etc. (Bilal *et al*., 2019). The above mentioned conventional methods were not up to the expectations because of the inability to perform complete mineralization, production of toxic by-products, unworthiness of biodegradation based treatments as pharmaceuticals are inherently toxic to biological species employed and their high cost. So, it becomes a necessity to develop new techniques for treatment of contaminated wastewater more effectively than conventional methods (Agnihotri *et al*., 2018). The focus is now being shifted towards the synthesis of novel materials at nanoscale. Among various non-conventional technologies used, Advanced Oxidation Processes (AOPs) became the most efficient technique for expulsion of contaminants from waste water. AOPs were accomplished to oxidize organic pollutants into intermediate species, that eventually turns into inorganic compounds through hydroxyl radicals ($OH^{\bullet}$) (Kanakaraju *et al*., 2018).These are further distinguished into various processes that are; photo-Fenton process, Fenton process, photo-induced process, ozonation, ultrasound, photo catalysis.

AOP based wastewater treatment performed using photocatalysis is done by the help of metal nanoparticles like TiO_2, ZnO, and other oxides which behave as effective catalysts for degradation. These nanoparticles consist of distinctive properties when compared to their bulk part, which involve its sole mechanical, optical, physical and the electromagnetic properties. The size, large surface area to volume ratio, shape, and mass dependent activity made these metal nanoparticles exceedingly photocatalytic in nature (Ghosh *et al*., 2002). Various routes of nanoparticle synthesis are studied among which chemical synthesis method has gained the maximum applicability due to its robustness, ease and better control over morphology, size and dispersity of nanoparticles.

Among several semiconductors studied for photocatalytic degradation process, titanium dioxide (TiO_2) became the most considered one because of its strong oxidizing power, non-toxicity, low cost and is easy to handle. But, the major disadvantage of using TiO_2 as an effective catalyst is its large band gap of 3.2 eV due to which it is active only under UV light that accounts for 10% of the solar spectrum. Also the rapid e^- and h^+ charge pair recombination reduces the degradation efficiency (Ni *et al*., 2007). So to make it work under solar spectrum, synthesized nanoparticles were doped with iron which reduced its band gap, making it visible light active (Sood *et al*., 2015). Further, to enhance the degradation rate, make its removal easy from slurry system the nanocomposite was loaded using biopolymers. Among various polymers such as chitosan, PVA (Polyvinyl acetate), cellulose, we prefer cellulose for loading (HPS *et al*., 2016) due to its abundance in nature and least expensive.

Therefore, in the recent study, an effort was made to synthesize cellulose functionalized Fe-TiO_2 bionanocomposite which was further evaluated for the photocatalytic degradation of methylene blue. Synthesized bionanocomposite is characterized through FTIR, DLS, ZP, DRS, XRD, SEM, EDX and BET to study the morphology, size and charge distribution of nanoparticles. Various parameters were performed in order to check the degradation efficiency of prepared catalyst which includes: pH, dye concentration, catalyst concentration, irradiation time, reusability test and scavenging effect on the catalyst in degradation experiments. Kinetic modelling followed by methylene blue degradation was also studied. Finally, the prepared bionanocomposite is used to check the degradation efficiency of pharmaceutically active compound i.e. diclofenac.

Objectives of the Project Work:

- Synthesis and characterization of Fe doped TiO_2 nanoparticles.
- Synthesis and characterization of cellulose functionalized Fe doped TiO_2 bionanocomposite.
- Photocatalytic degradation of model organic contaminant: Evaluation of process conditions and its optimization.

CHAPTER 2

Literature Review

The enormous growth in economy across globe resulted in rapid industrialization and hence water contamination through recalcitrant compounds. Recalcitrant compounds are referred as chemicals which are highly resistant to microbe degradation in both soil as well as water showing adverse effects even at micro levels (Pouran *et al*., 2015). The advancement in area of textile and medical science for providing colourful and safe life to humans raise the demand for dyes and pharmaceuticals (Tiwari *et al*., 2017). Dyes are coloured ionizing aromatic, heterocyclic compounds which show affinity towards the substrate, they are being applied to. In modern era, dyes are prepared from petroleum based intermediates and coal tars referred as synthetic dyes. The first synthetic dye ever prepared by human was Mauviene. Among different types of dyes such as acridine dyes, azo dyes, anthroqinone dyes, etc. azo dye i.e. Methylene Blue is found as the major contaminant. It is cationic, water soluble, thiazine dye a formal derivative of pentothiazine which works by converting the ferric iron in haemoglobin to ferrous iron (Rauf *et al*., 2011). With dyes, pharmaceuticals even after treatment, at low level (ng/L to mg/L) are detected frequently in drinking water, natural and wastewater bodies. These are the chemical compounds based on their therapeutic activity are categorized into diverse classes such as antibiotics, analgesic/antipyretics, central nervous system drugs, cardiovascular drugs, beta blockers and many more. Major source of their entrance into water streams include human urine where 90% of the drug gets released in un-metabolised form. Also the discard from hospitals, landfill leachates and veterinary waste becomes the reason for their mixing in water streams (Chauhan *et al*.,2019).

After China, India is among the second largest exporter of dye stuff. The size of Indian textile market is expected to reach up to US$ 223 by 2021 (IBEF 2019). During fabric manufacturing process around 10-15% of dye colorants are discarded off to water streams without any treatment. Along with dyes India is also the largest producer of generic drugs where India alone exports 20% of the global generic compounds (IBEF 2019). This sector of India alone provides about 17.27 billion USD in 2016-17 which is expected to increase by 20 billion USD by 2020. According to recent data report collected 36% increment in antibiotic consumption has been

observed in India (Chauhan *et al*., 2019). The ill effects caused by these compounds are headache, vomiting, confusion, shortness of breath, red blood cell breakdown and allergic reactions. Under long term contact of these compounds the colour of urine, sweat and stool changes from blue to green. Burning sensation in eyes had been observed leading to permanent damage (Agnihotri *et al*., 2018). In aquatic organisms, development of intersex fishes has been observed and also contributes to the development of antibiotic resistant strains. As consequences, it became essential to find out effective methods to eliminate these substances in surface and wastewater.

2.1 Conventional Wastewater Treatment Methods

The degradation rate and strategy of recalcitrant compounds mainly rely on biological and chemical nature of the compounds such as solubility, biodegradability, adsorption etc. In ancient time, conventional wastewater treatment was applied as a standard method to reduce harmful effects of wastewater. It is the fusion of three different processes (Figure1) i.e. physical, biological and chemical which help to remove solids, organic matter & nutrients from polluted water. The conventional wastewater treatment methods include: screening, mixing, flocculation, chemical precipitation, ion exchange, adsorption, activated sludge process, sludge digestion (Dariani *et al*., 2016). These methods have been tried to remove recalcitrant compounds, however they show some limitations of poor degradation efficiency due to:

- Production of secondary by-products after degradation which are toxic in nature.
- During sorption based treatment, the sorption ability of dyes and pharmaceutical contaminants affect the properties of sludge.
- Due to highly toxic nature of recalcitrant compounds towards the biological species, conventional method based on biological degradation is not effective.

With the overall knowledge of lethal effects of recalcitrant compounds and their inability of complete degradation through conventional wastewater treatment method, it became a necessity to develop better techniques based on nano-enabled hybrid technology which provides more effective degradation results.

2.2 Nanotechnology Based Treatment

Nanoscience and nanotechnology became the key for Research and Development with their increasing use in every field (Bystrzejewska *et al*., 2009). Nanotechnology is science carried out at nano scale (1-100 nm). The notion about nanotechnology started in a talk entitled as "There's Plenty of Room at the Bottom" by a well-known physicist Richard Feynman at the California Institute of Technology (CalTech) where American Physical Society meeting was been held on December 29, 1959, at times where nanotechnology term was still unknown. Here Feynman described an operation which aided scientists to manage and run particular atom and molecules. After certain years, while examining ultra-precision machining, other Professor named Norio Taniguchi incidentally gives the word nanotechnology. In 1981, when the scanning tunnelling microscope was developed which helps to "see" individuals atoms, become the reason for evolution of term nanotechnology (Khan *et al*., 2017). The achievements gained by researchers in area of nanotechnology found its practical applications in daily life, in industries and medicines as well. To tackle with recalcitrant compounds, nano-enabled techniques such as Advanced Oxidation Processes have gained immense importance (Figure1).

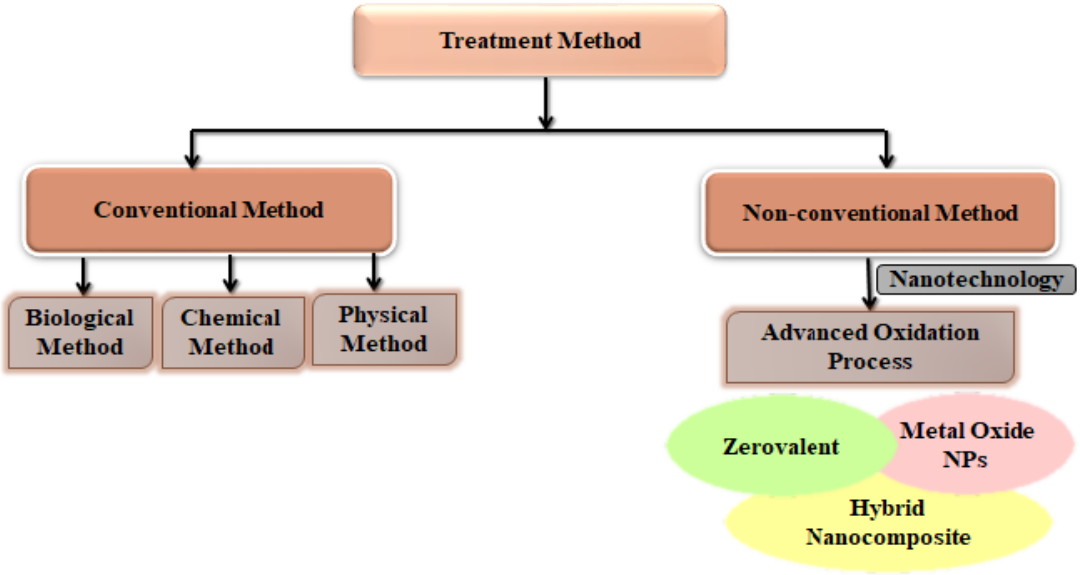

Figure 1: Schematic representation of various approaches for wastewater treatment

AOPs carry out degradation process based on production of reactive oxygen species and free radicals which degrade pollutants into simpler and toxic free components.

Radical species are termed as atoms or molecules with single unpaired electron present on them for e.g., hydroxyl radical ($HO^{\bullet}$), peroxide radical ($HO^{\bullet}_2$), superoxide anion radical ($O_2^{\bullet-}$), and alkyl radical ($RO^{\bullet}$), among which the hydroxyl radicals came out to be most effective in degradation process. The reason why hydroxyl radicals gain maximum attention is: its non-selective nature, powerful oxidizing capabilities (Eo = +2.80 V) and high reactivity. These $HO^{\bullet}$ radicals react with organic compounds through different reaction methods which can either be by hydrogen absence from C-H, N-H, or OH groups, also through radical-radical interactions, and by direct electron transfer hence giving oxidized intermediates. After complete mineralization of compounds, these AOPs produce CO_2 (carbon dioxide), H_2O (water) and inorganic acids. Despite of having maximum oxidizing capabilities, the degradation rate depends on the bond between $OH^{\bullet}$ and the organic pollutant.

$HO^{\bullet} + RH \rightarrow R^{\bullet}$ Eq. (1)

$R^{\bullet} + O_2 \rightarrow RO^{\bullet}_2$ Eq. (2)

$HO^{\bullet} + RX \rightarrow RX^{\bullet} + OH^{-}$ Eq. (3)

Some of the most commonly used AOPs for degradation of recalcitrant compounds involves UV, electrochemical oxidation, Photo-Fenton, sonolysis, ozonation, UV/peroxide oxidation, photocatalysis etc. (Kanakaraju *et al*., 2018).

2.3 Nanoparticle Synthesis

Substantially two approaches are mostly studied for synthesis of nanorange particles: "top to bottom" approach and "bottom to top" approach (Figure 2).

- Bottom to top approach – In this synthesis of nanoparticles occur through chemical or biological methods where nanoscale particles are formed by self-assembly of atoms.
- Top to bottom approach – In this technique size reduction of appropriate bulk material occurs through different approaches including grinding, milling etc. producing fine particles of nano scale.

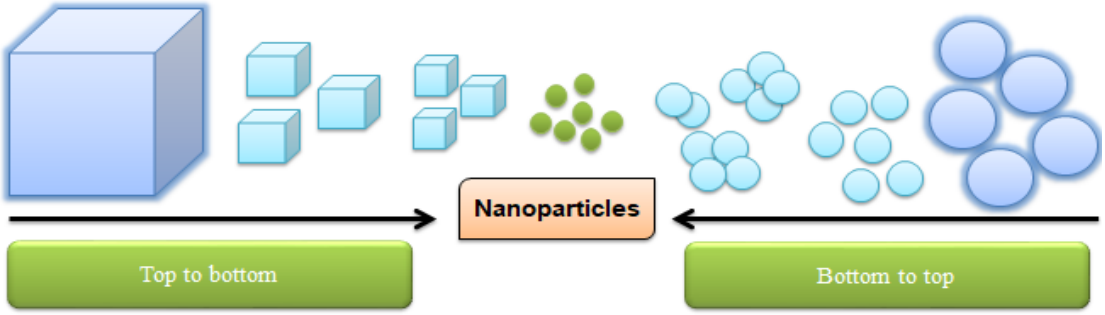

Figure 2: Approaches for synthesis of nanoparticles

The morphology and size of nanoparticles formed depends on technique used for their preparation. Mostly bottom-up approach is preferred for nanoparticle synthesis. This is classified under two different methods such as: chemical (supercritical fluid, use of inorganic matrix as support, and coprecipitation) and biological (which includes use of algae, fungi, bacteria, or plants) whereas physical process is carried out in synthesis on nanoparticle through "top to down" approach: (microwave irradiation, ultraviolet radiation, sonochemical, laser ablation, thermal decomposition, photochemical), Further, 2 types of techniques are followed during synthesis through physical method such as mechanical and vapour. Mechanical techniques include, melt mixing and ball milling whereas the vapour technique includes laser ablation, ion implantation, sputter deposition etc. When preparing nanoparticles through biological method, fungi, algae, plants, DNA (Deoxyribonucleic acid) etc. are utilized (Ahmed *et al*., 2016). Above all these techniques present, nanoparticle synthesis is carried out through chemical reduction which helps in synthesis of control sized NPs. Obtained nanoparticles when studied were found to be monodispersed and colloidal in nature. Some of the chemical methods include, sol-gel method, solution based method, chemical precipitation, template method synthesis. Rapid nucleation of nanoparticles is observed in this method providing us with small size nano-range particles.

2.4 Properties of Nanoparticles

Various forms of nanomaterial have been discovered such as nanotubes, nanowires, particles, films, quantum dots as well as colloids. Nano-range materials have properties different from their bulk properties where high surface-to-volume ratio of nanoparticles results in swift increase of reactivity occurring at molecular level. Materials at nanoscale

behave totally different when compared to bulk material but it is still difficult to study their chemical and physical properties. The surface and interfacial properties of nanoparticles get changed in presence of chemical reagents (Mueller & Nowack, 2010). Consequently, these reagents are the one which support the NPs against coagulation or aggregation by maintaining particle charge or through modification in its outmost layer. The characteristics of nanoparticles are based up on their inner and surface structures which include shape and size. NPs either interact with one other or could remain free based on attractive or repulsive interaction forces between them which make their characterization difficult. Ideal nanoparticles should have high surface area, fast dissolution, strong sorption and high reactivity. These also have some discontinuous properties referred to as super paramagnetism, quantum confinement effects and also localized surface plasmon. More is the presence of surface defects on nanoparticles, more effective is the photocatalyst. Due to formation of discrete energy levels nanoparticles blue shift has been observed in nanoparticles making them able to behave as atom individually.

2.5 Chemical Synthesis of Nanoparticles

With their unique chemical and physical characters, nanoparticles are used in diverse fields like industrial applications, health impacts, and environmental studies. Conventionally chemical method is preferred for synthesizing metal or metal-oxide nanoparticles which occur through alterations in basic properties (chemical, physical) of used precursor. The process of chemical synthesis start by selecting compounds referred as precursor which gets converted into atom after addition of chemical reductants. These synthesized atoms undergo the process of nucleation then aggregation and at last formation of nanoparticles. There are various sources for synthesis of metallic and other nanoparticles including precursors, ethanol, other chemicals using different techniques such as chemical precipitation, template method, hydrothermal method etc. Iron doped TiO_2 is synthesized through co-precipitation method, by ultrasonication and finally calcination. Sonochemistry has always been proved to be a good method in preparation of mesoporous materials that arises from detectable depressions, the formation, growth and later on implosive collapsing of bubbles into liquid (Stankic *et al.*, 2016). Calcination always performed in air is done for powders where the powdered material is heated at high temperature causing change in properties of nanoparticles. It is observed that a better scattering of the

nanoparticles, better thermal stability, higher surface area, and also phase clarity is obtained by sonication (Bagheri *et al*., 2015).

2.6 Photocatalysis

Heterogeneous photocatalysis is appearing to be valuable AOP for water purification and degradation of recalcitrant compounds. A semiconductor used as photocatalyst is identified on the basis of electronic structures present among which the one filled band with highest energy is stated as valence band (VB) whereas another empty one with low energy is referred as conduction band (CB). The gap that separates both these bands is called as band gap that has forbidden energy. When the radiation with energy equal or greater compared to that of the band gap energy is taken up by a semiconductor particle, the e^- from VB gets excited into CB which simultaneously generates h^+ in VB. These e^- and h^+ have ability to recombine at the outer surface or inner bulk of particle matter within a fraction of nanoseconds that causes dissipation of energy in form of heat. These electron/holes generated could also get trapped at surface states inside which these charges act with donor atoms (D) or acceptor atoms (A) species which are absorbed or found close to surface of particle. The energy level present at the bottom of CB is nothing but the reduction potential of photoelectrons whereas, energy level at top of VB gives the oxidizing ability of photo holes (Zaleska, 2008).

2.7 Nanomaterial in Photocatalysis

Photocatalysis is the operation of progress which includes converting organic contaminants into inorganic and toxic free compounds, generating CO_2 and H_2O with the use of catalyst and AOPs. The aqueous system of nature is typically purified through solar light which starts this breakdown of organic compounds. Degradation protocol carried out using photocatalysis doesn't produce any toxic compound, making it more valuable than any other AOP. The surrounding oxygen itself acts as required oxidant for photocatalysis. The attributes of model photocatalyst is that it should be non-toxic, stable, inexpensive and highly photoactive in nature. Nanoparticles act as photocatalyst that intensify the degradation rate. Most of the photocatalyst used are the semiconductors of metal oxides, ordinarily having a narrow band gap. These induce the radical species which further reacts with impurities in water and degrade them non-selectively. Titanium dioxide NPs are widely used as

heterogeneous photocatalysts due to some reasons such as: low cost, inertness, high refractive index as well as having photostable nature. The main reason for using TiO_2 as a catalyst is that it could be used in slurry as well as fixed bed reactors. The size range that generally desired is 20-50 nm. In nanoparticles, combined oscillations of electrons of conduction band (CB) results in Surface Plasmon Resonance (SPR) and these electrons resonate with the incident light (electromagnetic field). When these electrons settle to their thermal equilibrium states, they release heat in their surrounding which induce reaction in molecules that are adhered on the surface of nanoparticles (Figure 3). Since, TiO_2 is the most efficient catalyst used to carry out degradation process but it has some limitations as well such as:

- Photogenerated e^-/h^+ pair recombination: electrons from CB very quickly recombine with holes from VB and produce heat or photons.
- Rapid backward reaction between hydrogen and oxygen occurs causing formation of water which effects the production rate of free radical species and hence degradation rate.
- Due to large band gap of TiO_2 i.e. 3.2 eV it is able to work efficiently under UV radiations only. Since UV light is only about 5% - 10% of solar light whereas visible light is about 50% of solar light, hence reducing degradation efficiency (Ni *et al*., 2007).

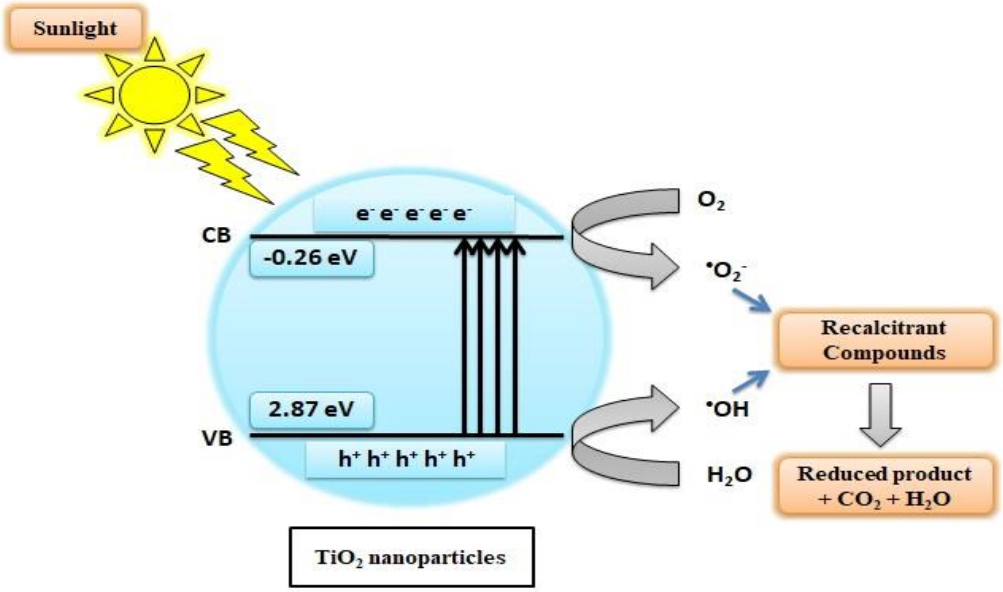

Figure 3: Mechanism of degradation of recalcitrant compounds using TiO_2 nanoparticles

In order to make the catalyst visible light active and resolve the above listed problems, continuous research is being carried out. For which doping of metals, non-metals or transition metals were experimentally performed and some among these were found to be effective in reducing band gap. Different dopants used for this process includes: Ag, C, N, Fe, V, Cu, Co, Au, and Pt etc. (Figure3). Out of all metal doping is the most opted one as the benefits associated with it are:

- Inhibition of electron – hole pair recombination.
- Threshold wavelength response increases in visible region.
- Generation of heterojunctions.
- Formation of new discontinuous energy level beneath the CB thus reducing band gap.

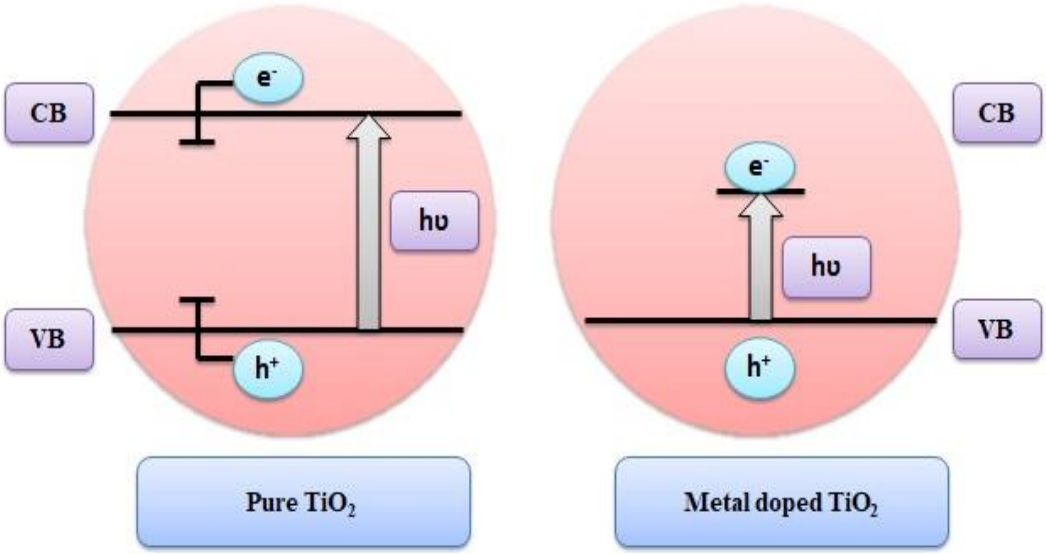

Figure 4: Effect of metal doping on TiO_2

Among various metal dopants Fe is found to be the most effective dopant because of:

- Same ionic radii of Fe^{3+} (0.693A°) which is nearly same as that of Ti^{4+} (0.745A°).
- Stable half-filled d^5 electronic configuration of Fe.
- Fe^{3+} acts as charge carrier trap, hence inhibiting e^-/h^+ pair recombination (Ali *et al*., 2017).

Fe doped TiO_2 shows overlapping between d orbital of Ti and d orbital of Fe^{3+} which make these nanoparticles more efficient to carry out degradation under solar light (Figure 4).

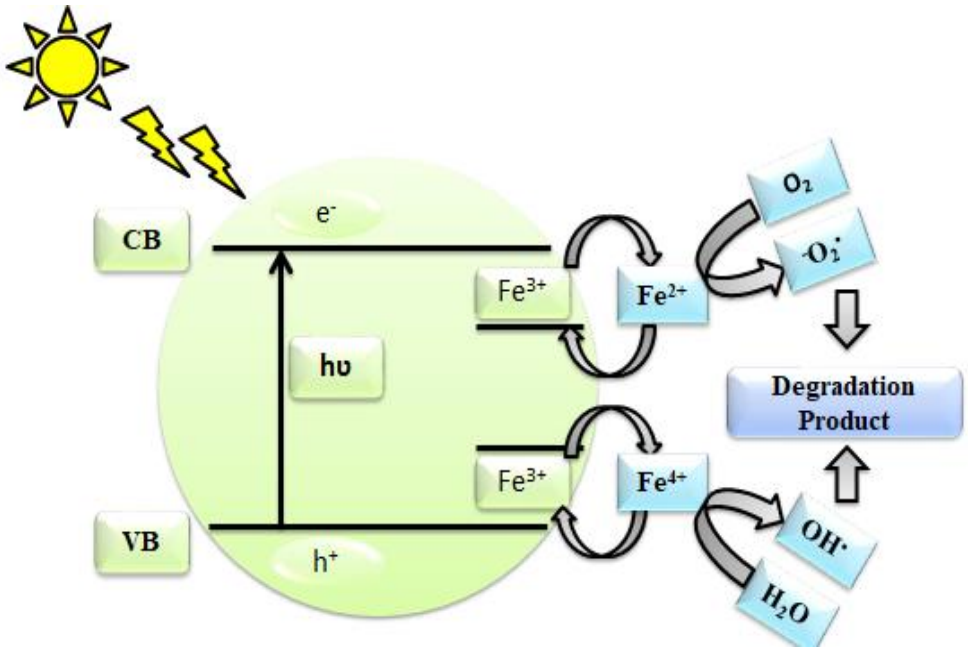

Figure 5: Photocatalytic mechanism of Fe-TiO_2 nanoparticles

2.8 Immobilization of Fe doped TiO_2 Nanoparticles on Cellulose

Biopolymers are the support matrix having flexible nature, mechanically stability, low cost, easy availability and high durability. Biopolymers including cellulose and chitosan have appeared as an efficient material to carry out the adsorptive removal of dyes and other heavy metals from contaminated water (Olivera *et al*., 2016). Cellulose is the most abundant biopolymer found on earth and is naturally obtained from plant sources such as wheat stalks, recycled newspapers, wood, grass, sugarcane bagasse, bacteria, fungi etc. (HPS *et al*., 2016). It is renewable, natural, non-toxic and biodegradable in nature. The advances occurring in nanoscience has provided us with the possibility to develop nano-sized cellulose which became an attractive option because of its surface properties, ease of functionalization and chemical accessibility. Cellulose immobilized TiO_2 NPs are easy to remove from the treated solution through adsorption and filtration techniques thus providing us clean water (Olivera *et al*., 2016).

There are various literatures shown in Table 1 representing the degradation of MB and pharmaceutical compounds by Fe doped TiO_2 NPs and other cellulose based bio composites.

Table 1: Literature survey for evaluation of various photocatalyst for degradation of dyes and PhACs

Photocatalyst	**Target Compound**	**Light Source & Time Required**	**% Degradation**	**References**
TiO_2	Ibuprofen	UV radiations, 240 minutes	99%	Jallouli *et al*., 2018
TiO_2	Venlafaxine	UV irradiations, 30 minutes	99%	Lambropoulou *et al*., 2017
Fe-TiO_2	MO	300 W Halogen Tungsten, 360 minutes	72%	Tong *et al*., 2008
Fe-TiO_2	Pentoxifyllin	Solar spectrum, 180 minutes	92%	Bansal *et al*., 2018
Cellulose acetate-Fe films	Reactive Black 5	Solar Radiation, 180 minutes	86%	Ribeiro *et al*., 2016
RC/N-doped TiO_2	Phenol	Under UV as well as Visible light for 180 minute	96.6%&78.8% respectively	Mohamed *et al*., 2016
BC/TiO_2	Methylene Blue	Philips(125W), 35 minutes	89%	Brandes *et al*., 2018
TiO_2 Cellulose	Paracetamol	UV irradiation, 120 minutes	79%	Baeza *et al*., 2019

*MO – Methylene Orange, TiO_2 – Titanium dioxide, UV – Ultraviolet radiations,

BC – Bacterial Cellulose, RC – Regenerated Cellulose, Fe – Iron, TiO_2 – Titanium dioxide

2.9 Characterization techniques

2.9.1 X-Ray Diffraction (XRD)

XRD helps to observe the crystallite and amorphous quality of synthesized nanoparticles along with purity of sample. The sample is homogenized properly in a solvent and the pattern was noted under Bragg's angle (θ). Debye Scherrer formula is used to calculate the average particle size:

$$D=0.9\lambda\beta\cos\theta$$

Where, D is thickness of nanoparticle, β is half maxima of reflection at Bragg's angle 2θ, λ is referred as wavelength of X-ray & θ reflects the diffraction angle or Bragg's angle. X-Ray produce scattered beams after striking on single nanoparticle crystal forms a diffraction pattern.

2.9.2 UV-Visible Spectrophotometric Analysis

This technique helps in determining the organic and inorganic components present in any solution. It works on the principle of Beer-Lambert law which says, when a beam of monochromatic light passes through solution having an absorbing substance, the rate at which radiation intensity decreases is directly proportional to concentration of solution and incident radiation i.e.

$$A = \log (I_0/I)$$

Where: A is absorbance, I_0 is intensity of light upon a sample cell and I is the intensity of light departing the sample cell. As light falls on matter, electrons get excited providing optical band gap.

2.9.3 Dynamic Light Scattering (DLS) Analysis

Dynamic light scattering (DLS) assists to discover size distribution pattern of nanoparticles. The principle behind this technique is Brownian motion of molecules and particles in suspension scattered the laser of light at different intensities. Measurement of these fluctuations of intensities can be used to analyse the Brownian motion velocity and size of particle by Stoke – Einstein relationship. The equation is given as:

$$D_h = \frac{k_B T}{3\pi\eta D_t}$$

Where: D_h shows the hydrodynamic diameter of nanoparticle, D_t gives us the translational diffusion coefficient, k_B is the Boltzmann's constant, T denotes the thermodynamic temperature and η shows the dynamic viscosity. In DLS, these fluctuations can be measured by photon counter.

2.9.4 Scanning Electron Microscope (SEM) Analysis

SEM helps in the production of sample images by scanning the surface of sample through focused electron beams. The principle at which SEM works depends on the interactions that take place between the sample and electron beam predicting results at various magnifications. It is carried out after the sample is completely air dried. The sample is loaded with metal and is kept on sample holder. After which focused beam is used to scan the sample and produce images.

2.9.5 Fourier-Transform Infrared Spectroscopy (FTIR)

This technique is used to determine the functional groups present on the nanoparticles. This work on the principle that when infrared radiation of 10,000 to 100 cm^{-1} are passed through the sample, few radiations get absorbed whereas some of these get passed away. These radiations when get adsorbed, gets converted into rotational and vibrational energies. When IR radiations get on the surface on nanoparticles the molecular fingerprint of sample is generated. Each single sample has its own unique fingerprint which helps to identify the chemicals present in the sample.

2.9.6 Brunaer-Emmett-Teller (BET) Analysis

BET analysis serves as the basis for analysing specific surface area of materials. This theory only applies to system of multilayer adsorption and uses gases referred as probing gas which doesn't react with material surface in order to detect specific surface area. Among various gases used, liquid nitrogen is mostly preferred and is carried out at boiling temperature of N_2 gas which is 77 K. This concept is based on Langmuir theory, which was given for monolayer molecular adsorption. Specific surface area calculated through this technique depends on adsorbate molecule used and its cross-section.

CHAPTER 3

Materials and Methods

3.1 Materials

Titanium n-butoxide ($Ti(OCH_2CH_2CH_2CH_3)_4$) was purchased from Sigma-Aldrich; absolute ethanol (99.9%) ; iron chloride hexahydrate, ($FeCl_3.6H_2O$), microcrystalline cellulose and urea were purchased from Loba Chemie; NaOH and methylene blue (MB) dye powder were procured from SD Fine-chemicals. Magnetic stirrer model MS H280 Pro and Centrifuge model himac CR 22G were used; pestle mortar and sonicator were also used. All glasswares were washed using aqua regia solution and distilled water. These were kept for drying at 60°C and stored in dry conditions for further use.

3.2 Preparation of Titanium Dioxide Nanoparticles (TiO_2)

2.5 ml of titanium butoxide and 25 ml of ethanol was taken in a beaker while 13 ml of distilled water and 13 ml of ethanol were taken in another round bottom flask. Both the solutions were mixed in round bottom flask under constant stirring of 30 minutes. This resulted in formation of white suspension which was collected after centrifugation at 4000 rpm for 20 minutes. The pellet obtained was washed using ethanol and distilled water properly after which it was oven dried at 100°C (Li *et al*., 2008).

3.3 Preparation of Fe-TiO_2 Nanoparticles

An appropriate stoichiometric amount of iron chloride hexahydrate was added to 25 ml of distilled water to synthesise 0.5% Fe-TiO_2. The resultant solution was then stirred at 1000 rpm for 2-3 hours followed by sonication for 1 hour. The yellow coloured product obtained was then dried and calcined at 100°C and 400°C respectively.

3.4 Immobilization of Fe-TiO_2 Nanoparticles on Microcrystalline Cellulose

4 wt% of cellulose solution was prepared by adding appropriate amount of cellulose into another solution containing NaOH, urea and distilled water in the ratio 7:12:81. The prepared slurry was precooled at -20°C and thawed extensively to obtain an

almost transparent solution. To this solution 25 mg of iron doped TiO_2 was added and left for sonication for about 2 hours till it properly gets dispersed. The obtained suspension was centrifuged for 20 minutes at 3000 rpm. The formed pellet was finally washed with distilled water and dried for further photocatalytic applications (Mohamed *et al*., 2015).

3.5 Preparation of MB Solution

40 ppm of methylene blue stock was prepared by adding 4 mg of MB powder in 100 ml of distilled water with continuous stirring for 5 min. The working MB solutions were subsequently prepared over a wide range of 5 - 20 ppm (5, 10, 14, 16, 18) from the stock solution of 40 ppm.

3.6 Photocatalytic Decolourisation of MB Dye

The photocatalytic decolourisation of organic pollutant i.e. MB dye was done with the chemically synthesized cellulose-Fe doped TiO_2 NPs. The reaction was carried out by mixing 1.6 mg/ml of prepared catalyst in 10 ml of dye solution in a glass batch reactor. The adsorption-desorption reaction was performed for about 40-45 minutes by keeping samples in the dark after which they were placed in direct sunlight under continuous stirring conditions. At every interval of 20 minutes 200µl of sample was retrieved and its decolourization kinetics was studied using UV–Visible spectrophotometer till it gets properly degraded which took around 120 minutes. The decolourization percentage was calculated by the formula:

$$\text{Decolourization (\%)} = \frac{\text{Co}-\text{C}}{\text{Co}} \times 100 \qquad \text{Eq. (4)}$$

Where, C is final concentration of dye and C_0 is initial concentration of dye.

3.7 Optimization of Dye Decolourization

Single Factor Study

To determine the various factors affecting the dye decolourization single factor study was performed. To carry out this study, the factors taken into account were: (A) effect of pH, (B) effect of dye concentration, (C) effect of catalyst, (D) effect of irradiation time, (E) effect of various scavengers, (F) reusability test

A. Effect of pH – 20 ppm dye solution was prepared with different pH, i.e. 4, 6, 7, 8, 10 and 1.6 mg/ml of catalyst was added to each vial. UV-Visible spectrophotometric readings were recorded after 2 hours.
B. Effect of dye concentration (ppm) – Dye solution was prepared with different concentrations of 10, 20, 30, 40 ppm having 1.6 mg/ml of catalyst and was mixed well. UV–Visible spectrophotometric readings were taken after 2 hours.
C. Effect of catalyst – 20 ppm dye solution was prepared and 10 ml was taken into different glass vial. To this different concentration of catalyst i.e. 0.4 mg/ml, 0.8 mg/ml, 1.6 mg/ml was mixed properly. Then UV–Visible spectrophotometric readings were recorded after 2 hours.
D. Effect of irradiation time – 20 ppm was prepared to which 1.6 mg/ml of catalyst was added and mixed properly. UV–Visible spectrophotometric readings were recorded after 0, 10, 20, 40, 60, 80, 100, 120 min.
E. Reusability test – 20 ppm of dye was prepared and 1.6 mg/ml of catalyst was added to it, mixed well. Degradation rate was observed for constitutive 8 readings with same parameters after 2 hours daily.

3.8 Kinetic Modelling

Photocatalytic decolourization of dye can be more precisely described by kinetic modelling, models are known as decay models. For practical application of photocatalytic reaction, kinetic models are necessary. In this study, four different kinetic models were made to analyse the photocatalytic degradation of MB by TiO_2 NPs.

1) First-order kinetic model (Equation 5)

$$\ln[Co - C] = -kt \qquad \text{Eq. (5)}$$

2) Pseudo First-order kinetic model (Equation 6)

$$\ln[Co - C] = \ln[C] - kt \qquad \text{Eq. (6)}$$

3) Second-order kinetic model (Equation 7)

$$\frac{1}{C} - \frac{1}{Co} = kt \qquad \text{Eq. (7)}$$

4) Pseudo Second-order kinetic model (Equation 8)

$$\frac{t}{C} = \frac{t}{Co} - \frac{1}{kC^2} \qquad \text{Eq. (8)}$$

3.9 Preparation of Standard Curve for Diclofenac

100 ppm of diclofenac stock was prepared by adding 50 mg of drug was dissolved in 500 ml of distilled water with continuous stirring for 10-15 minutes. From this 100 ppm stock solution the working diclofenac concentrations were prepared over wide range from 5-20 ppm i.e. 5, 10, 14, 16, 18, 20 ppm. After preparation of standard its absorbance was noted at 340 nm.

3.10 Photocatalytic Degradation of Diclofenac

The photocatalytic degradation of organic pollutant i.e. diclofenac was done with the chemically synthesized cellulose immobilized Fe doped TiO_2 NPs. The reaction was carried out by spiking 10 ml of distilled with 2 mg of drug and 10 mg of bionanocomposite is added to the above prepared solution in a glass batch reactor. The adsorption desorption process was performed for about 40-45 minutes by keeping samples` in the dark after which they were placed in direct sunlight under continuous stirring conditions. At every interval of 20 minutes 200µl of sample was retrieved and its degradation kinetics was studied using UV – Visible spectrophotometer till it gets properly degraded which took around 120 minutes. The degradation percentage was calculated by the formula:

$$\text{Decolourization (\%)} = \frac{\text{Co} - \text{C}}{\text{Co}} \times 100 \qquad \text{Eq. (9)}$$

Where, C is final concentration of dye and C_0 is initial concentration of dye.

- All the experimental work was carried out from months between March to June between 11 am to 1 pm.

CHAPTER 4

Results and Discussion

4.1 Characterization of Synthesized Nanoparticles

4.1.1 Scanning Electron Microscope (SEM) Analysis

The SEM images of Fe doped TiO_2 nanoparticles immobilized on cellulose support matrix are shown in figure 6. Results of SEM analysis carried out at different magnifications shows equal distribution and incorporation of Fe doped TiO_2 nanoparticles at the surface of microcrystalline cellulose indicating the presence of strong bond which arises because of electrostatic or chemical interactions. Cellulose interactions with TiO_2 NPs prevent the alteration and morphology of bionanocomposite during different reaction conditions (Virkutyte *et al*., 2012).

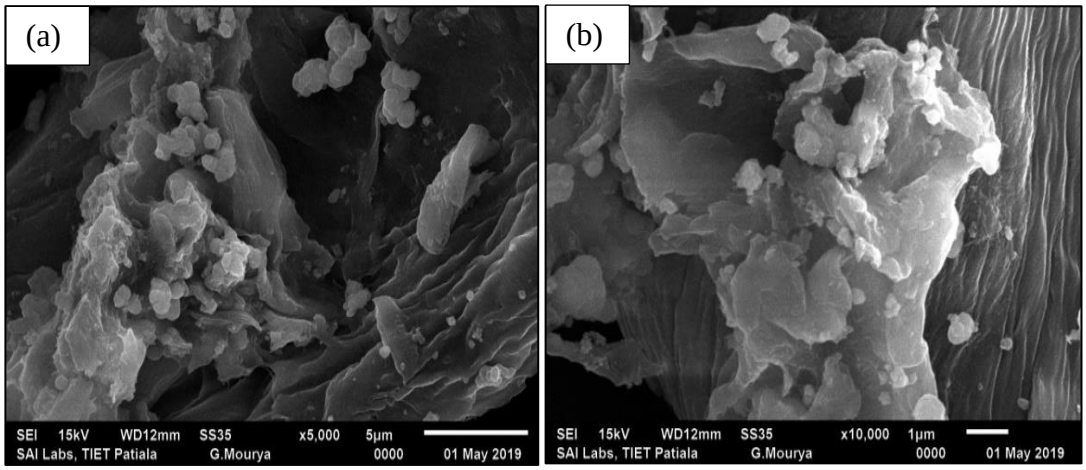

Figure 6: SEM micrographs of Fe doped TiO_2 nanoparticles immobilized on cellulose (a) at 5,000x and (b) at 10,000x

4.1.2 Energy Dispersive X-ray spectroscopy (EDX) Analysis

Table 2 illustrates different elements present in Fe doped TiO_2 nanoparticles immobilized on microcrystalline cellulose based on the weight and atomic percentage and figure 7 represents the EDX plot of SEM images of Fe-TiO_2-cellulose bionanocomposites. The EDX result shows different intense peaks present at Ti, O, Fe and C atoms.

Table 2: Elemental composition of synthesized bionanocomposite

Elements	Weight %	Atomic %
C K	41.91	51.06
O K	51.22	46.85
Ti K	6.69	2.05
Fe K	0.18	0.05

Fe atoms on doping enter the lattice of TiO_2 nanoparticles. Presence of C and O atom occurs due to the use of microcrystalline cellulose in preparation of bionanocomposite. The composition of elements in bionanocomposite is in agreement with those proposed in preparation progress.

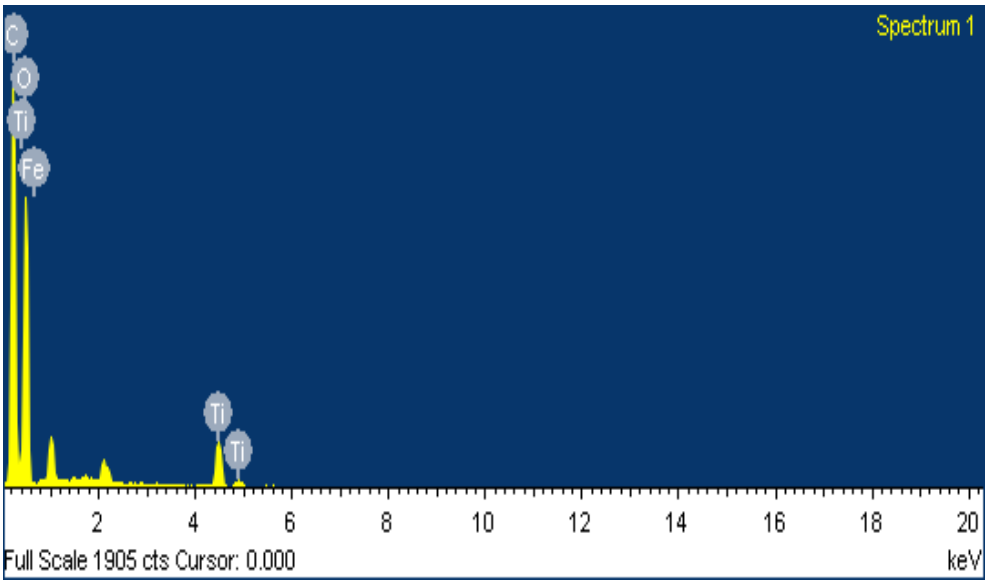

Figure 7: EDX plot of Fe doped TiO_2 nanoparticles immobilized on microcrystalline cellulose

4.1.3 Dynamic Light Scattering (DLS) and Zeta Potential Analysis

DLS analysis is carried out to find the hydrodynamic diameter of synthesized bionanocomposite. With DLS, Zeta Potential was also carried out to check the charge present on the sample as shown in figure 8 and figure 9. Zetasizer Nano ZS equipment was used for determination of particle size and charge of nanoparticles dispersed in Milli Q water. From figure 8 it was found that the hydrodynamic diameter was 434 nm and poly dispersity index of 0.583.

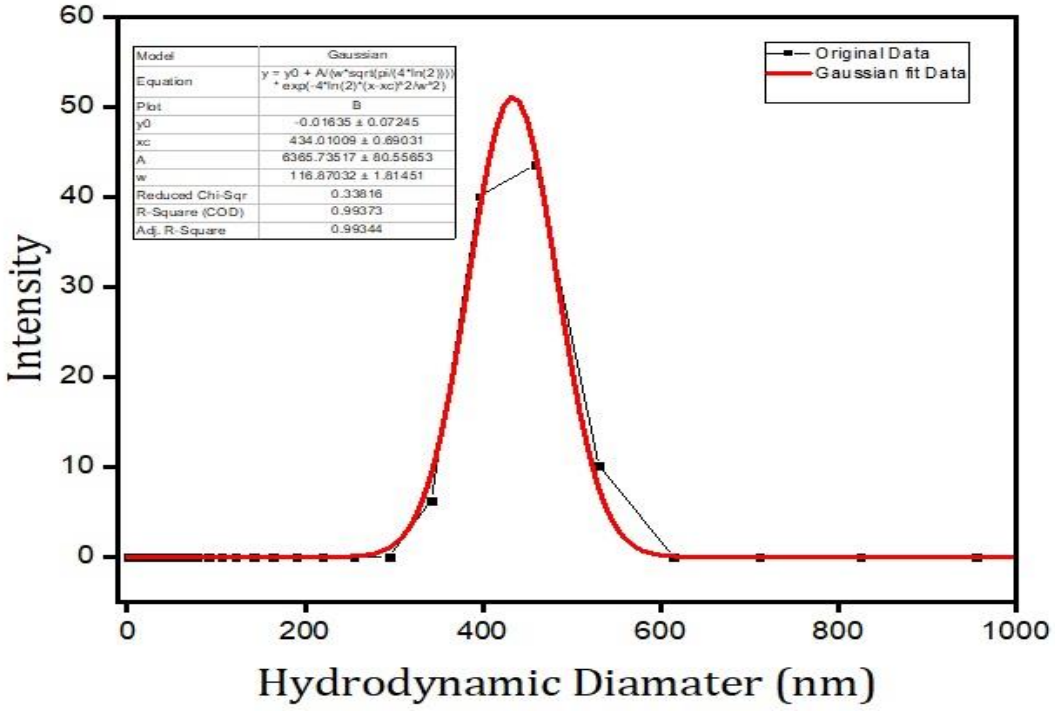

Figure 8: DLS analysis of cellulose immobilized Fe doped TiO_2

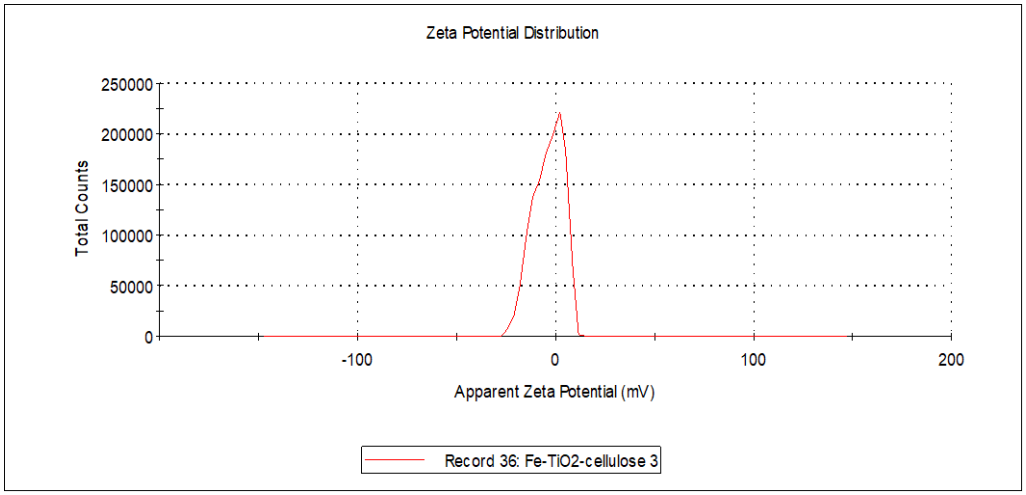

Figure 9: Zeta potential curve of the synthesized bionanocomposite

The stabilities of dispersion were observed with zeta potential of -3.80 mV which represent the premises of well dispersed nanoparticles. This negative charge on the surface indicates that the bionanocomposite synthesized is capable of adsorbing cationic dye at its surface and hence enhancing its degradation rate.

4.1.4 Diffuse Reflectance Spectroscopy (DRS) Analysis

0.5 wt. % doping of Fe on TiO_2 NPs was performed which were further immobilized on microcrystalline cellulose. The prepared bionanocomposite was subjected to DRS measurement in order to compare the reduction in band gap and enhancement in degradation rate.

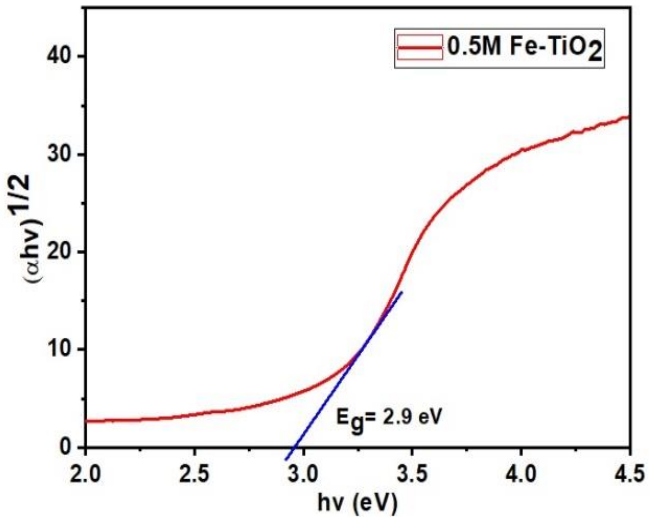

Figure 10: Tauc plot of Fe-TiO_2 nanoparticles

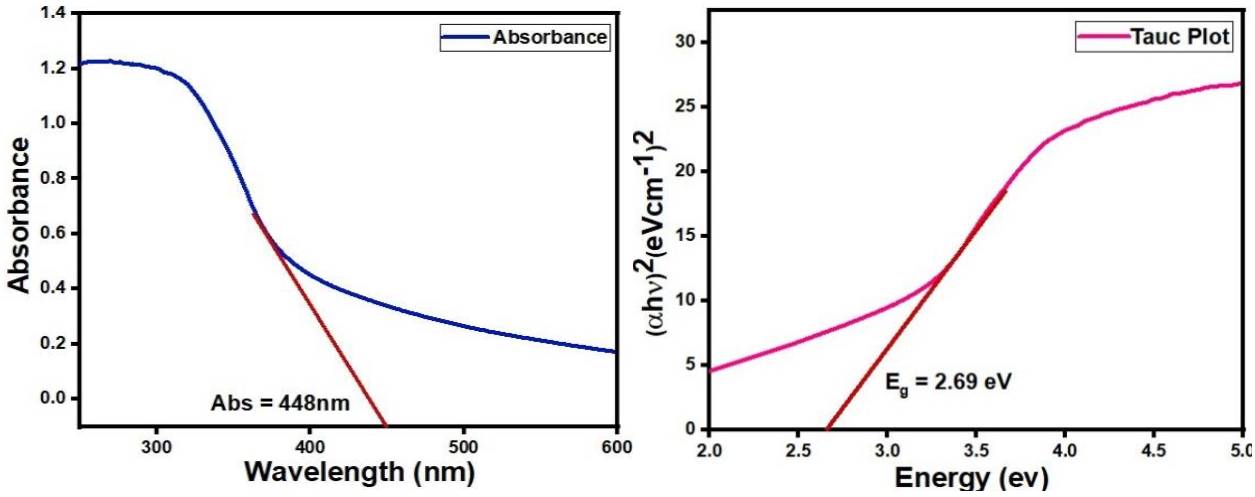

Figure 11: Absorbance and Tauc plot of Fe doped TiO_2 nanoparticles immobilized on microcrystalline cellulose

From obtained results it was evident that Fe doping was necessary to reduce the band gap and enhance photodegradation. The figure 10 shows that band gap reduces from 3.2 eV to 2.9eV when doping is performed as iron get incorporated into the lattice structure of TiO_2 altering its electronic configuration. Moreover, Fe doping results in lowering of e^- and h^+ pair recombination which results in enhanced photoadsorption of O_2. Based on touc plot in figure 11 further reduction in band gap was observed from 2.9eV to 2.69eV in case of Fe-TiO_2-cellulose causing a red shift in absorption. This red shift in adsorption edge of Fe doped TiO_2 attributed to the excitation of 3d electrons of TiO_2 to Fe conduction band (charge-transfer transition).

4.1.5 Brunauer-Emmett-Teller (BET) Analysis

N_2 physical adsorption-desorption isotherms helps to determine the surface area and pore size diameter of Fe doped TiO_2 nanoparticles and bionanocomposite prepared through immobilization of these nanoparticles on cellulose. The BET isotherm and relative to this the BJH plot obtained from the adsorption branch of isotherm of the catalyst are represented in figure 12.

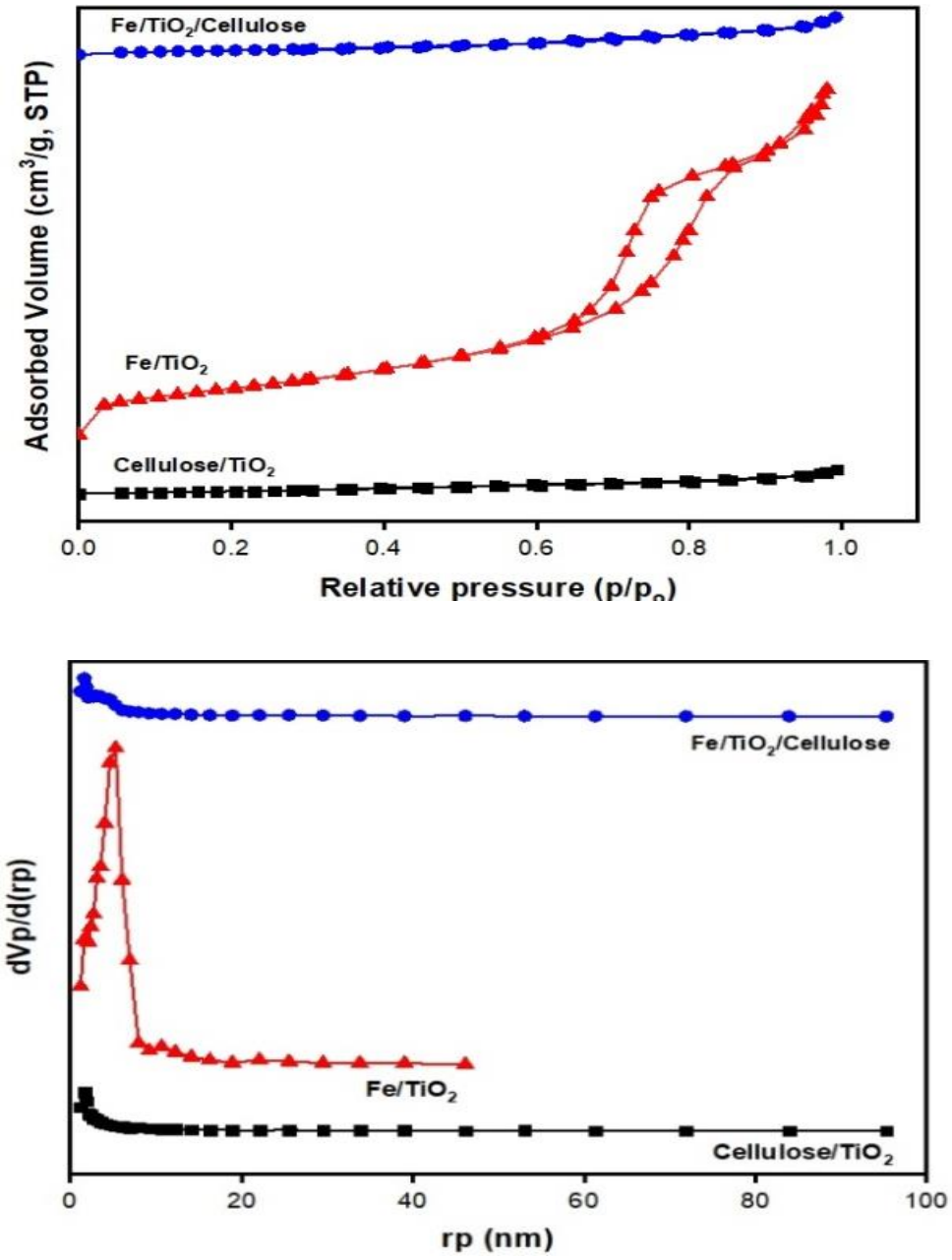

Figure 12: (a) Adsorption-Desorption isotherms of Fe doped TiO_2 nanoparticles and bionanocomposite

(b) BJH plot of Fe-TiO_2 nanoparticles and bionanocomposite

The BJH plot tells us about the pore size of cellulose-TiO_2, Fe-TiO_2 nanoparticles and cellulose immobilized Fe doped TiO_2 confirming the presence of mesoporous structures as depicted in table below.

Table 3: Representation of specific surface area, pore diameter and pore volume of nanocomposites and bionanocomposite

	Fe-TiO_2	**Cellulose-TiO_2**	**Cellulose immobilized Fe-TiO_2**
Specific Surface Area	72.329 (m^2/g)	6.4949 (m^2/g)	7.1562 (m^2/g)
Mean Pore Diameter	11.147 (nm)	8.3422 (nm)	11.91 (nm)
Total Pore Volume	0.2016 (cm^3/g)	0.0135 (cm^3/g)	0.021308 (cm^3/g)

As concluded from Table 3 the decrease in specific surface area of Fe-TiO_2 i.e. 72.329 (m^2/g) to 7.1562 (m^2/g) on adding cellulose to nanocomposite occurs due to increase in agglomeration on top layer of nanoparticles and also inside the bulk of adsorbent matrix. This agglomeration occurs because the vacant spaces found in cellulose get filled by Fe-TiO_2 during synthesis. The increase in mean pore diameter of cellulose immobilized Fe-TiO_2 reflects the high porosity of cellulose.

4.1.6 X-Ray Diffraction (XRD) Analysis

XRD analysis was carried out to find the crystalline properties of cellulose, the synthesized Fe-TiO_2-cellulose bionanocomposite and micro-structural changes occurred. The XRD pattern of cellulose and synthesized Fe-TiO_2-cellulose is shown in figure 13. XRD study shows the characteristic peaks of pure cellulose which appeared at 2θ value of 23.1° and 35° were for (200) and (044) respectively, corresponds to the structure of plane particles. Neither a new peak nor any peak shit was observed when compared with pure cellulose indicates that Fe-TiO_2-cellulose bionanocomposite consists of two phase structures i.e. nanoparticles as well as polymer. The diffraction peak at 2θ value of 23.9° were for (101) represents the anatase phase of bionanocomposite. This result indicates that addition of cellulose to nanocomposite causes overall increase in crystallinity which affects the final properties of bionanocomposite (Ahmadizadegan, 2017).

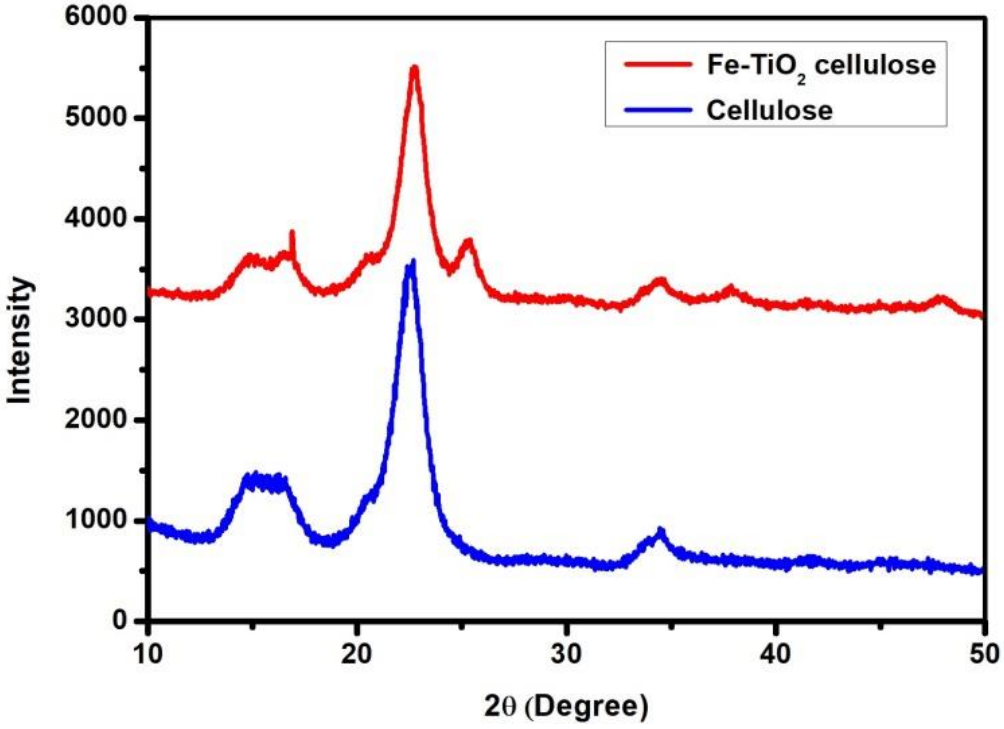

Figure 13: XRD plot of pure cellulose and bionanocomposite

4.1.7 Fourier-Transform Infrared Spectroscopy (FTIR)

FTIR of Fe-TiO_2-cellulose was recorded in wavenumber ranging between 4000-500 cm^{-1}. The FTIR spectrum of bionanocomposite has been shown in figure 14 having well defined peaks. The peak at 3345.8 cm^{-1} shows the absorption of surface OH bond in cellulosic composite (Sood *et al.*, 2015). The peak at 1629 cm^{-1} shows the H-O-H bending vibration of absorbed water. From this it was concluded that addition of Fe ions in TiO_2 matrix results in changes which enhance absorption of OH groups. The peak observed at 2901 cm^{-1} shows the stretching of C-H bond. The band appearing at 668 cm^{-1} and 560 cm^{-1} refers to Ti-O stretching modes of Ti-O-Ti or may be due to vibration of anti-symmetric Ti-O-Ti modes of TiO_2 (Ali *et al.*, 2017).

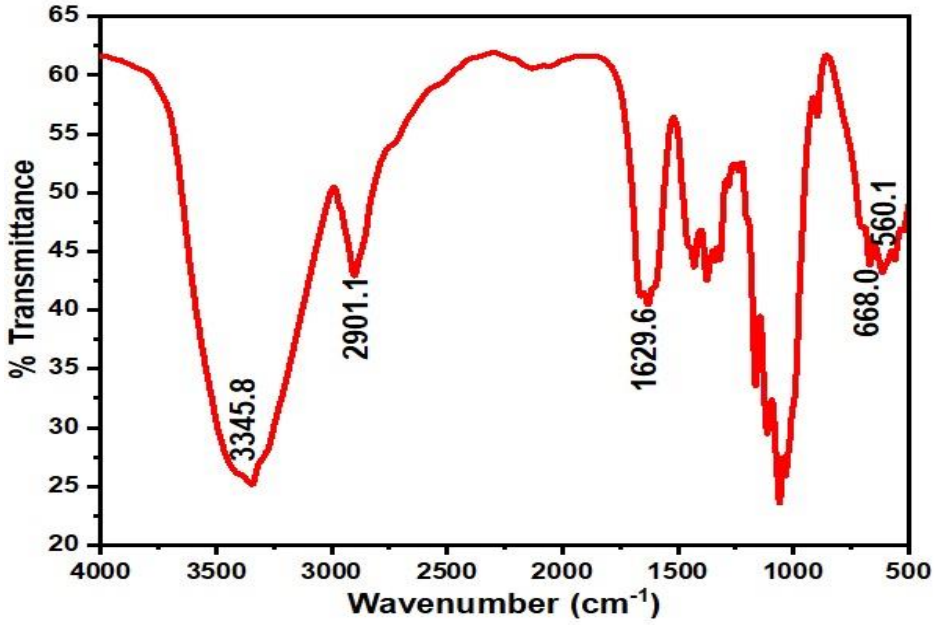

Figure 14: Typical FTIR spectra of as prepared Fe-TiO_2 Cellulose

4.2 Standard Curve of Methylene Blue

Standard curve for methylene blue dye was prepared from the stock solution of 20 ppm having concentrations: 5, 10, 14, 16, 18 and 20 ppm. Their absorbance was taken in UV–Visible spectrophotometer at 664 nm.

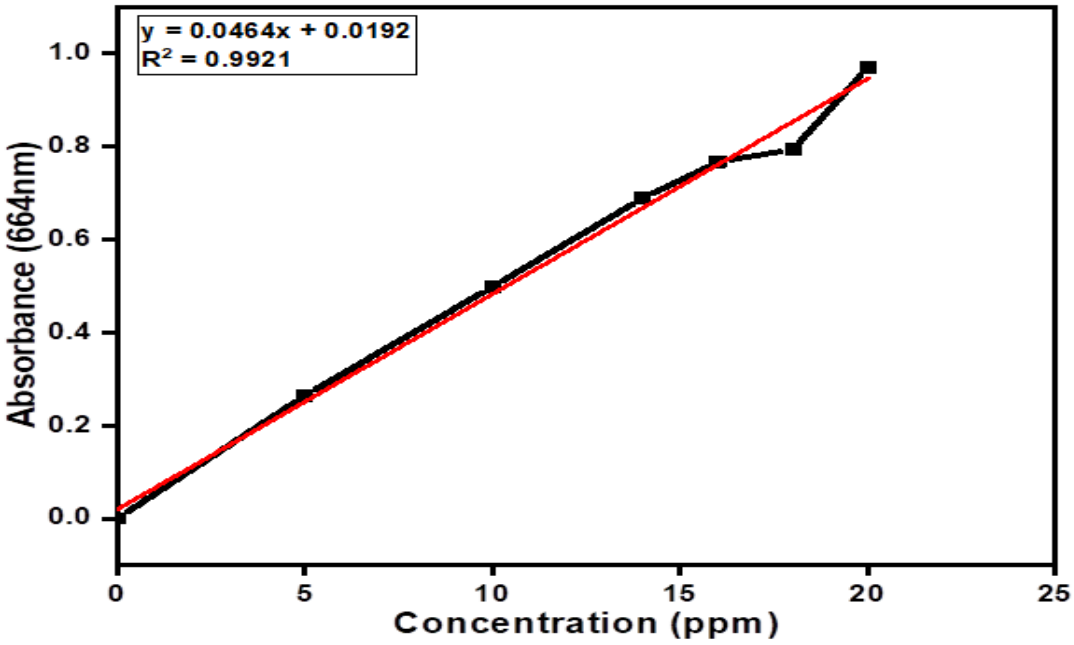

Figure 15: Standard curve representation of methylene blue dye

4.3 Single Factor Studies

The effect of different parameters on methylene blue degradation was studied; optimizing four different parameters i.e. dye concentration (ppm), catalyst concentration (mg/ml), irradiation time (minutes) and pH.

4.3.1 Effect of Dye Concentration

The photocatalytic degradation of MB was evaluated over particular range of dye concentration starting from 5ppm to 40 ppm under solar irradiation of 120 minutes. When checking out the effect of dye concentration it was observed that with continuous increase in concentration from 5 ppm to 20 ppm the photodegradation efficiency gradually reduces from 98% to 93.9% as shown in figure 16 (b). But as the concentration reaches up to 40 ppm a sharp reduction in degradation rate was observed i.e. 77%. The reason accounting for such fall in degradation rate is that MB is light sensitive in nature and with increasing dye concentration the layering of dye over the surface of nanoparticle also increases which hinders the direct contact of sunlight with bionanocomposite. Subsequently the number of hydroxyl radical attacking MB decreases dropping down the degradation rate. Thus the 20 ppm dye was found to be optimum to carry out further experiments (Tayeb & Hussein, 2015).

4.3.2 Effect of Catalyst Concentration

The effect of synthesized bionanocomposite on methylene blue was studied under 120 minutes of reaction time. The most effective degradation of methylene blue was observed at 1.6 mg/ml of catalyst concentration. The result shows that for catalyst concentration of 0.4, 0.8 and 1.6 mg/ml of 20 ppm dye solution the degradation rates are 77%, 85% and 95% respectively. The reason for this observation is that with increased catalyst concentration higher fraction of dye molecules get attached at the surface of bionanocomposite enhancing photo-oxidation reactions for degradation. However any further increase in catalyst concentration results in nanoparticle aggregation minimizing degradation efficiency. Also the ability of light to penetrate deep inside the solution with high catalyst dosage reduces because multiple backscattering of light decreases the overall adsorption of light at catalyst surface (Tayeb & Hussein, 2015).

4.3.3 Effect of pH

Another parameter studied was pH ranging from 4 to 10 for 120 minutes under solar illumination. pH is one of the most important factor that affects the photocatalytic degradation. It shows its promising effect on both the catalyst and dye solution during degradation experiment as the degradation rate depends on the surface charge present on catalyst i.e. positive, negative or neutral. The photocatalytic degradation proportion of MB exploiting synthesized bionanocomposite increases constantly on increase in pH showing maximum degradation at pH 10 i.e. 97%. This was the optimum pH condition at which the further experiments were carried out in whole study. This effect of pH on photocatalytic degradation is described as follows. The surface of bionanocomposite is negatively charged which generate more hydroxyl anions at high pH. These generated anions show electrostatic interaction with cationic dyes and adsorb more dye for degradation. Whereas in acidic pH more positive site surfaces are formed that don't tend to adsorb dye molecules and hence show less degradation efficiency (Benhabiles *et al*., 2016).

4.3.4 Effect of Irradiation Time

Effect of irradiation time was observed on decolorization efficiency up to 120 minutes time interval. In graph 16 (d), 95% degradation was observed up to 120 minutes which increases with more adsorption of catalyst with time generating excess of electrons and holes to carry out degradation.

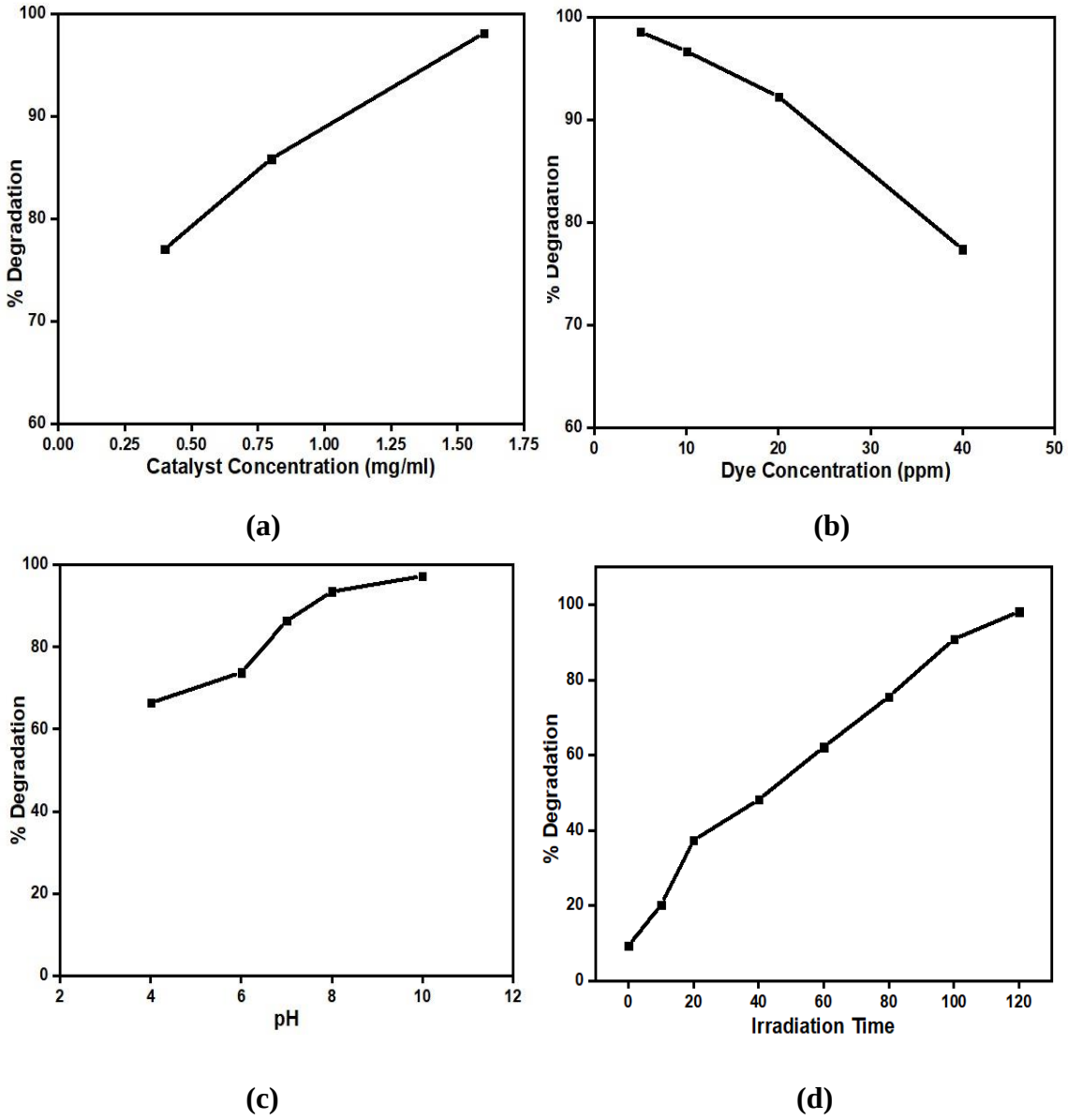

Figure 16: Graphs showing percentage degradation of MB dye at different (a) catalyst concentration, (b) dye concentration, (c) pH and (d) irradiation time

4.4 Effect of Scavengers

Generally, degradation of recalcitrant compounds through photocatalysis is result of the oxidative properties of reactive species generated that includes $^{\bullet}OH$, h^{+}, e^{-}, $^{\bullet}O_2^{-}$. The formation of $^{\bullet}OH$ and $^{\bullet}O_2^{-}$ radicals under light carries out degradation. The effect of scavengers was studied on photocatalytic degradation of Methylene Blue using four different scavengers where Methanol was used for hydroxyl radicals, Ascorbic Acid was used for hole radicals, p-benzoquinone was used for superoxide radicals and

Sodium Nitrate was used for e^- radicals. Photodegradation results show reduction in degradation efficiency on adding scavengers which occurs due to decrease in concentration of reactive oxygen species. This proves that hydroxyl and superoxide ($^{\bullet}OH$ & $^{\bullet}O_2^-$) radicals play vital role in photocatalytic degradation process. From figure 17 effects of scavengers was concluded on photocatalytic degradation. It was found that methanol inhibits the degradation and reduces it up to 45% and on addition of ascorbic acid it reduces up to 57%. This is due to the reason that h^+ generated during photo-oxidation reacts with H_2O to form hydroxyl radicals which play the most important role to carry out degradation at maximum rate. When these h^+ and hydroxyl radicals got scavenged the degradation rate decreases. But on addition of p-benzoquinone and sodium nitrate not much effect was observed in degradation percentage reduction. This is because of the fact that superoxide radicals are less stable when compared to hydroxyl radicals and react less with organic contaminants independently, so affecting less on degradation rate when scavenged. This concludes that degradation of Methylene Blue occurs through oxidation process majorly via attack by OH radicals (Soliman *et al.*, 2017)

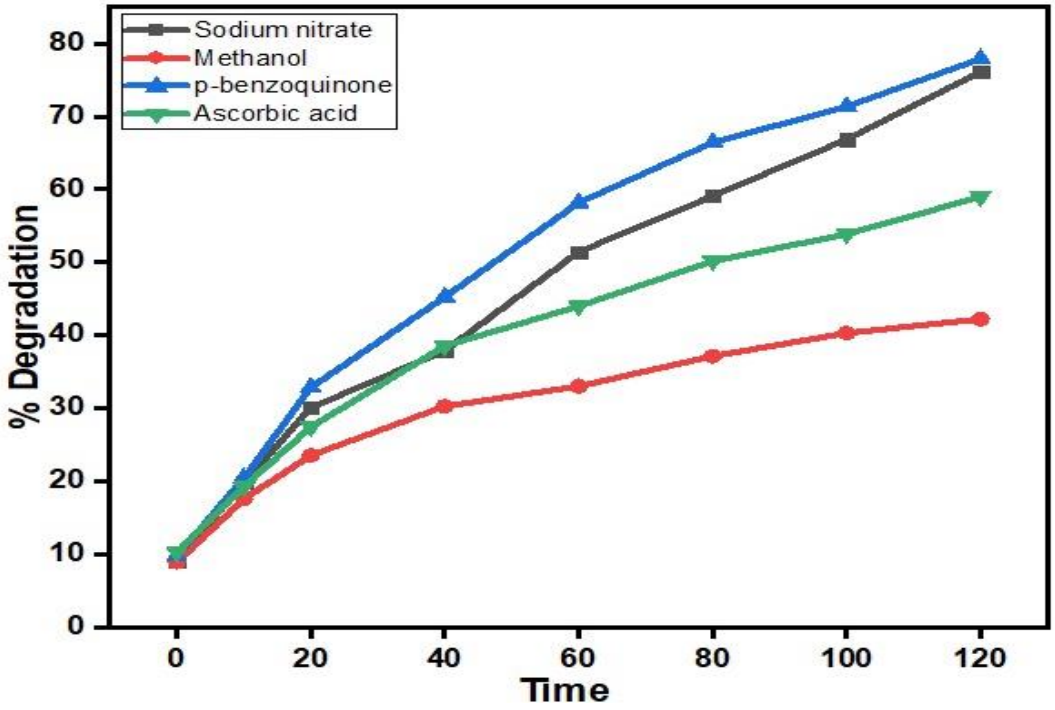

Figure 17: Effect on percentage degradation of MB dye after addition of different scavengers

4.5 Reusability Test

Recycling of photocatalyst is one of the main targets of industries which make the degradation process cost-effective. To study the reusability of photocatalyst, the catalyst was recycled 8 times regularly and degradation efficiency was plotted. These degradations were carried out at optimized conditions where 1.6 mg/ml of catalyst was added in 20 ppm of MB dye. The catalyst was recovered by washing it 2-3 times with distilled water and drying at optimum temperature. The dried catalyst is further reused to carry out degradation experiments. From figure 18 it was observed that degradation rate decreases from 95% to 49%. This reduction occurs due to constant loss of bionanocomposite on washing (Sarkar *et al*., 2015). Another reason for decrease in degradation rate may be that the surface of catalyst got covered by dye molecules which reduce the light reaching the catalyst hence decreasing the concentration of photo-generated holes and electrons.

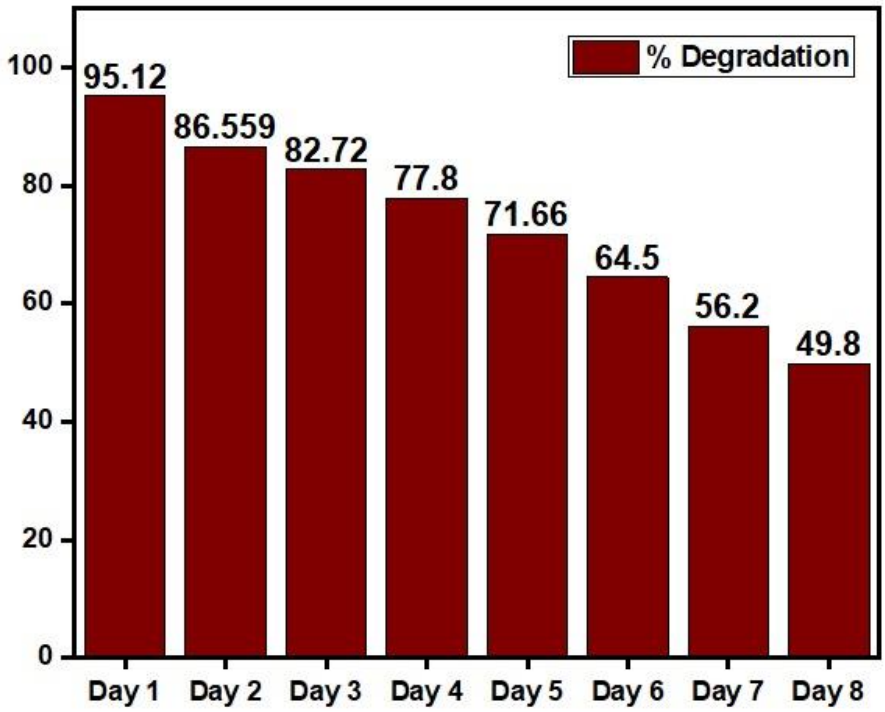

Figure 18: Effect on degradation percentage after reusing the sample

4.6 Kinetic Modelling

To understand the degradation mechanism of dyes under solar spectrum, kinetics was studied on the basis on Langmuir-Hinshelwood isotherm models. Four different types of kinetic models were studied i.e. first-order, pseudo-first order, second-order and

pseudo second-order showing results for model fitting in figure 19. The values of coefficient R^2 are also mentioned in figures and the order of kinetics followed by MB depends on the R^2 value. Among all models, it was concluded that degradation follows pseudo-first order kinetics in concordance with Langmuir equation shown as:

$$\ln (C_0\text{-}C) = kt$$

where C_0 is initial dye concentration and k is rate constant.

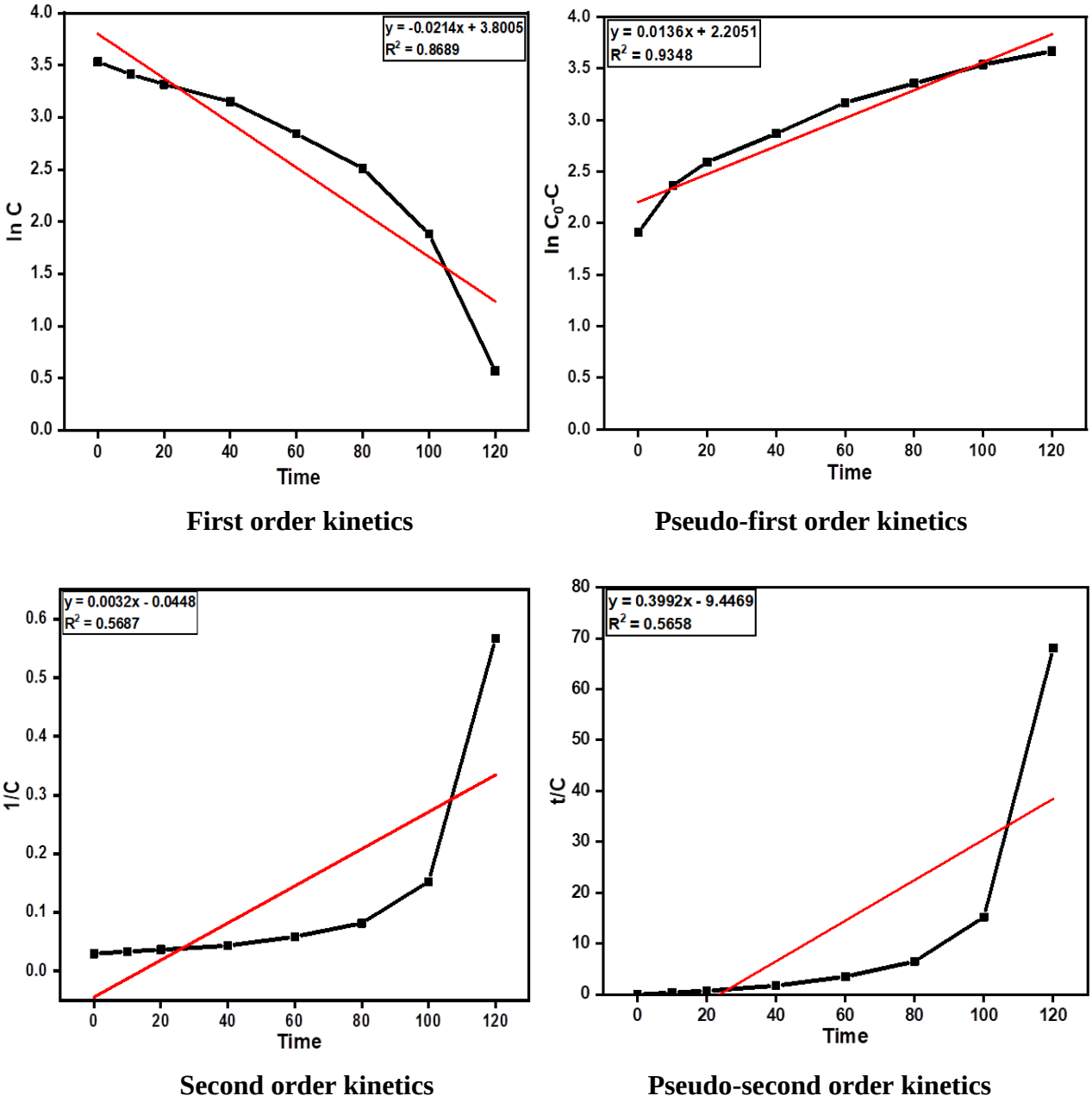

First order kinetics **Pseudo-first order kinetics**

Second order kinetics **Pseudo-second order kinetics**

Figure 19: Representation of kinetic model followed by MB dye

The linear correlation between C_0-C vs time which clearly proves that MB degradation follows pseudo-first order kinetics. Further the regression coefficient R^2 was found to be 0.9348 and intercept equal to zero which shows that degradation rate only depends on concentration of dye. Whereas, the R^2 value found in second order and pseudo-second order were far away from unity, which states that these models were not fit to depict degradation rate.

4.7 Standard Curve of Diclofenac

Standard curve for diclofenac was prepared from the stock solution of 100 ppm having concentrations: 5, 10, 14, 16, 18 and 20 ppm. Their absorbance was taken in UV–Visible spectrophotometer at 340 nm.

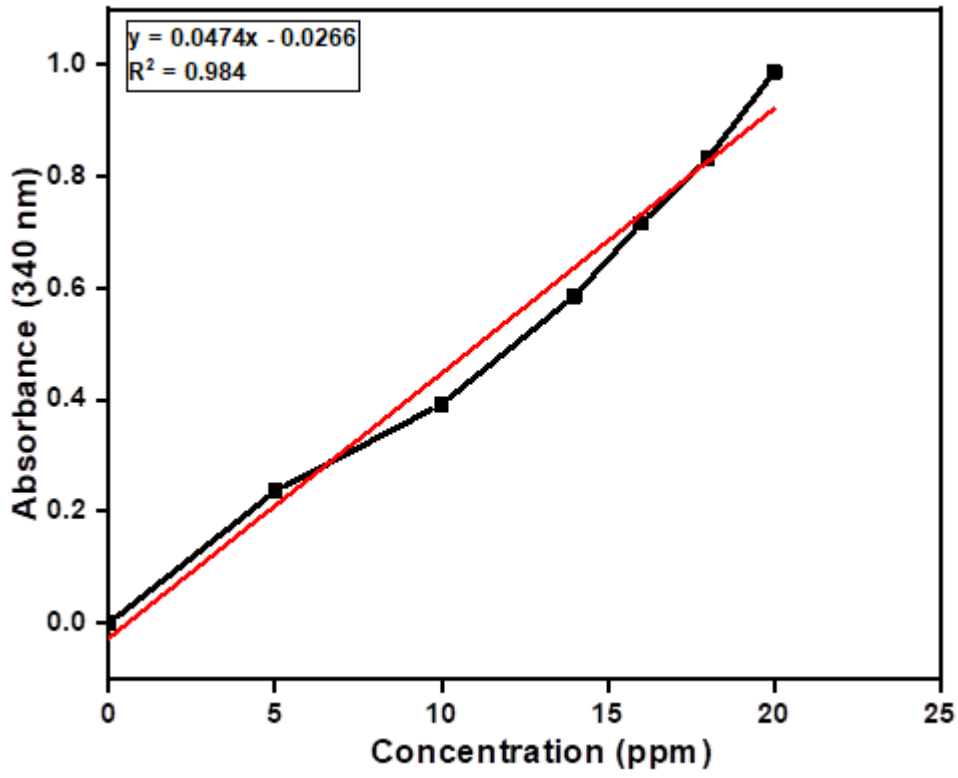

Figure 20: Standard curve of diclofenac

4.8 Photocatalytic Degradation of Diclofenac

Degradation of diclofenac was carried out for 120 minutes of irradiation time using synthesized Fe-TiO_2-cellulose bionanocomposite. To carry out this experiment 20 ppm of drug solution was prepared. 200µl of sample was extracted at different

intervals of 0, 10, 20, 40, 60, 80, 100 and 120 to find the degradation efficiency through UV-Visible spectrophotometer. The percentage degradation of Diclofenac was found to be 83.76% after 120 minutes and is represented in graph below.

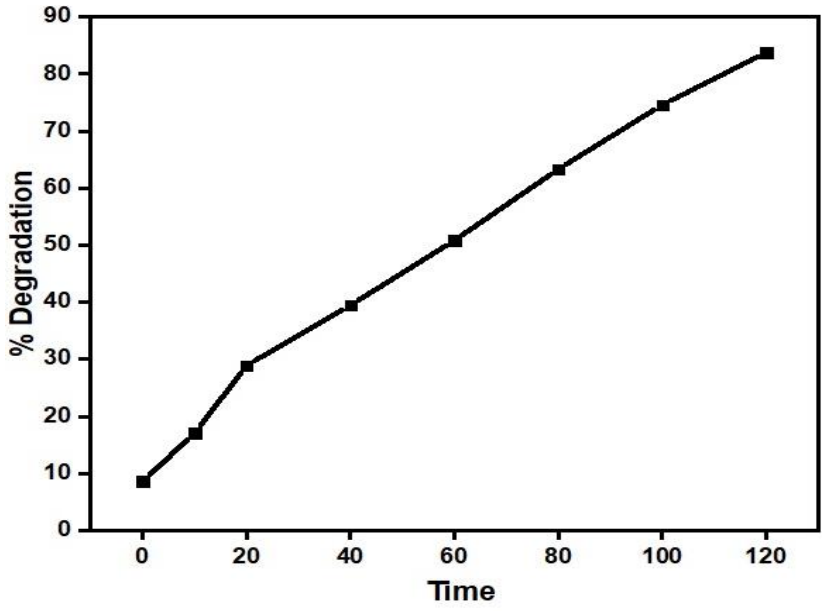

Figure 21: Graph representing percentage degradation of diclofenac

These anti-inflammatory drugs such as diclofenac are found to retain in water for longer time without being degraded through microorganisms. These compounds affect the water quality at large scale making it toxic and unfit for humans. The bionanocomposite prepared was capable of degrading 83.76% of diclofenac from wastewater reducing its harmful effects on humans and aquatic organisms. Further analysis of bionanocomposite could be helpful in degradation of other pharmaceutical compounds as well.

CONCLUSIONS

Heterogeneous photocatalysis was performed successfully to carry out degradation of model organic pollutants i.e. methylene blue and diclofenac using synthesized Fe doped TiO_2 nanoparticles mixed with microcrystalline cellulose. The degradation efficiency was found to be dependent on various parameters such as catalyst concentration, dye concentration, pH and irradiation time. Photocatalytic experiment concluded that maximum of 95% degradation was achieved for 20 ppm methylene blue dye as initial concentration with1.6 mg/ml catalyst concentration, pH 10 and 120 minutes of solar irradiation. Further reusability study over 8 consecutive cycles claimed the gradual decrease in degradation rate up to almost half i.e. (49%) on 8^{th} use, which predicts the cost-effectiveness of the used bionanocomposites. When observed under different scavengers, degradation rate reduces in the order of p-benzoquinone > sodium nitrate > ascorbic acid > methanol. Different kinetic studies performed reveals that MB follows pseudo-first order kinetics. This synthesized bionanocomposite was further used to check its efficiency for degradation of pharmaceutical active compound i.e. diclofenac under solar irradiation which shows 83% of drug degradation in 120 minutes. Thus, Fe-TiO_2-cellulose bionanocomposite based on above performed experiments appears to be an effective catalyst for degradation of organic contaminants at large scale.

REFERENCES

- Agnihotri, S., Sillu, D., Sharma, G., & Arya, R. K. (2018). Photocatalytic and antibacterial potential of silver nanoparticles derived from pineapple waste: process optimization and modeling kinetics for dye removal. *Applied Nanoscience*, *8*(8), 2077–2092.
- Ahmadizadegan, H. (2017). Surface modification of TiO_2 nanoparticles with biodegradable nanocellulose and synthesis of novel polyimide/cellulose/TiO_2 membrane. *Journal of Colloid and Interface Science*, *491*, 390.
- Ahmed, S., Ahmad, M., Swami, B. L., & Ikram, S. (2016). A review on plants extract mediated synthesis of silver nanoparticles for antimicrobial applications: a green expertise. *Journal of Advanced Research*, *7*(1), 17–28.
- Ali, T., Tripathi, P., Azam, A., Raza, W., Ahmed, A. S., Ahmed, A., & Muneer, M. (2017). Photocatalytic performance of Fe-doped TiO_2 nanoparticles under visible-light irradiation. *Materials Research Express*, *4*(1), 15022.
- Baeza, P., Aballay, P., Matus, C., Camú, E., Ramirez, M. F., Eyzaguirre, J., & Ojeda, J. (2019). Degradation of Paracetamol Adsorbed on Inorganic Supports Under UV Irradiation. *Water, Air, & Soil Pollution*, *230*(2), 34.
- Bagheri, S., Hir, Z. A. M., Yousefi, A. T., & Hamid, S. B. A. (2015). Progress on mesoporous titanium dioxide: Synthesis, modification and applications. *Microporous and Mesoporous Materials*, *218*, 206–222.
- Bansal, P., & Verma, A. (2018). In-situ dual effect studies using novel Fe-TiO_2 composite for the pilot-plant degradation of pentoxifylline. *Chemical Engineering Journal*, *332*, 682–694.
- Benhabiles, O., Mahmoudi, H., Lounici, H., & Goosen, M. F. (2016). Effectiveness of a photocatalytic organic membrane for solar degradation of methylene blue pollutant. *Desalination and Water Treatment*, *57*(30), 14067–14076.
- Bilal, M., Adeel, M., Rasheed, T., Zhao, Y., & Iqbal, H. M. (2019). Emerging contaminants of high concern and their enzyme-assisted biodegradation-A review. *Environment International*, *124*, 336–353.
- Brandes, R., Trindade, E. C., Vanin, D. F., Vargas, V. M., Carminatti, C. A.,

Al-Qureshi, H. A., & Recouvreux, D. O. (2018). Spherical Bacterial Cellulose/TiO_2 Nanocomposite with Potential Application in Contaminants Removal from Wastewater by Photocatalysis. *Fibers and Polymers*, *19*(9), 1861–1868.

- Bystrzejewska-Piotrowska, G., Golimowski, J., & Urban, P. L. (2009). Nanoparticles: their potential toxicity, waste and environmental management. *Waste Management*, *29*(9), 2587–2595.
- Chauhan, A., Sillu, D., & Agnihotri, S. (2019). Removal of Pharmaceutical Contaminants in Wastewater Using Nanomaterials: A Comprehensive Review. *Current Drug Metabolism*, *19*(00), 1-23.
- Dariani, R. S., Esmaeili, A., Mortezaali, A., & Dehghanpour, S. (2016). Photocatalytic reaction and degradation of methylene blue on TiO_2 nano-sized particles. *Optik*, *127*(18), 7143–7154.
- Ghosh, S. K., Kundu, S., Mandal, M., & Pal, T. (2002). Silver and gold nanocluster catalyzed reduction of methylene blue by arsine in a micellar medium. *Langmuir*, *18*(23), 8756–8760.
- HPS, A. K., Saurabh, C. K., Adnan, A. S., Fazita, M. N., Syakir, M. I., Davoudpour, Y., Dungani, R. (2016). A review on chitosan-cellulose blends and nanocellulose reinforced chitosan biocomposites: Properties and their applications. *Carbohydrate Polymers*, *150*, 216–226.
- Jallouli, N., Pastrana Martinez, L. M., Ribeiro, A. R., Moreira, N. F., Faria, J. L., Hentati, O., & Ksibi, M. (2018). Heterogeneous photocatalytic degradation of ibuprofen in ultrapure water, municipal and pharmaceutical industry wastewaters using a TiO_2/UV-LED system. *Chemical Engineering Journal*, *334*, 976–984.
- Kanakaraju, D., Glass, B. D., & Oelgemöller, M. (2018). Advanced oxidation process-mediated removal of pharmaceuticals from water: A review. *Journal of Environmental Management*, *219*, 189–207.
- Khan, I., Saeed, K., & Khan, I. (2017). Nanoparticles: Properties, applications and toxicities. *Arabian Journal of Chemistry*, 1878-5352.
- Lambropoulou, D., Evgenidou, E., Saliverou, V., Kosma, C., & Konstantinou, I. (2017). Degradation of venlafaxine using TiO_2/UV process: kinetic studies, RSM optimization, identification of transformation products and toxicity

evaluation. *Journal of Hazardous Materials*, *323*, 513–526.

- Lee, C. M., Palaniandy, P., & Dahlan, I. (2017). Pharmaceutical residues in aquatic environment and water remediation by TiO_2 heterogeneous photocatalysis: a review. *Environmental Earth Sciences*, *76*(17), 611.
- Li, Z., Shen, W., He, W., & Zu, X. (2008). Effect of Fe-doped TiO_2 nanoparticle derived from modified hydrothermal process on the photocatalytic degradation performance on methylene blue. *Journal of Hazardous Materials*, *155*(3), 590–594.
- Moctezuma, E., Leyva, E., Aguilar, C. A., Luna, R. A., & Montalvo, C. (2012). Photocatalytic degradation of paracetamol: Intermediates and total reaction mechanism. *Journal of Hazardous Materials*, *243*, 130–138.
- Mohamed, M. A., Salleh, W. N. W., Jaafar, J., Ismail, A. F., Mutalib, M. A., & Jamil, S. M. (2015). Incorporation of N-doped TiO_2 nanorods in regenerated cellulose thin films fabricated from recycled newspaper as a green portable photocatalyst. *Carbohydrate Polymers*, *133*, 429–437.
- Mueller, N. C., & Nowack, B. (2010). Nanoparticles for remediation: solving big problems with little particles. *Elements*, *6*(6), 395–400.
- Ni, M., Leung, M. K. H., Leung, D. Y. C., & Sumathy, K. (2007). A review and recent developments in photocatalytic water-splitting using TiO_2 for hydrogen production. *Renewable and Sustainable Energy Reviews*, *11*(3), 401–425.
- Olivera, S., Muralidhara, H. B., Venkatesh, K., Guna, V. K., Gopalakrishna, K., & Kumar, Y. (2016). Potential applications of cellulose and chitosan nanoparticles/composites in wastewater treatment: A review. *Carbohydrate Polymers*, *153*, 600–618.
- Pouran, S. R., Aziz, A. R. A., & Daud, W. M. A. W. (2015). Review on the main advances in photo-Fenton oxidation system for recalcitrant wastewaters. *Journal of Industrial and Engineering Chemistry*, *21*, 53–69.
- Rauf, M. A., Meetani, M. A., & Hisaindee, S. (2011). An overview on the photocatalytic degradation of azo dyes in the presence of TiO_2 doped with selective transition metals. *Desalination*, *276*(1–3), 13–27.
- Ribeiro, K., de Andrade, T. M., & Fujiwara, S. T. (2016). Preparation and application of cellulose acetate/Fe films in the degradation of Reactive Black 5

dye through photo-Fenton reaction. *Environmental Technology*, *37*(13), 1664–1675.

- Sarkar, S., Chakraborty, S., & Bhattacharjee, C. (2015). Photocatalytic degradation of pharmaceutical wastes by alginate supported TiO_2 nanoparticles in packed bed photo reactor (PBPR). *Ecotoxicology and Environmental Safety*, *121*, 263–270.
- Soliman, A. M., Elsuccary, S. A. A., Ali, I. M., & Ayesh, A. I. (2017). Photocatalytic activity of transition metal ions-loaded activated carbon: Degradation of crystal violet dye under solar radiation. *Journal of Water Process Engineering*, *17*, 245–255.
- Sood, S., Umar, A., Mehta, S. K., & Kansal, S. K. (2015). Highly effective Fe-doped TiO_2 nanoparticles photocatalysts for visible-light driven photocatalytic degradation of toxic organic compounds. *Journal of Colloid and Interface Science*, *450*, 213–223.
- Stankic, S., Suman, S., Haque, F., & Vidic, J. (2016). Pure and multi metal oxide nanoparticles: synthesis, antibacterial and cytotoxic properties. *Journal of Nanobiotechnology*, *14*(1), 73.
- Tayeb, A. M., & Hussein, D. S. (2015). Synthesis of TiO_2 nanoparticles and their photocatalytic activity for methylene blue. *American Journal of Nanomaterials*, *3*(2), 57–63.
- Teh, C. M., & Mohamed, A. R. (2011). Roles of titanium dioxide and ion-doped titanium dioxide on photocatalytic degradation of organic pollutants (phenolic compounds and dyes) in aqueous solutions: A review. *Journal of Alloys and Compounds*, *509*(5), 1648–1660.
- Tiwari, B., Sellamuthu, B., Ouarda, Y., Drogui, P., Tyagi, R. D., & Buelna, G. (2017). Review on fate and mechanism of removal of pharmaceutical pollutants from wastewater using biological approach. *Bioresource Technology*, *224*, 1–12.
- Tong, T., Zhang, J., Tian, B., Chen, F., & He, D. (2008). Preparation of Fe^{3+}-doped TiO_2 catalysts by controlled hydrolysis of titanium alkoxide and study on their photocatalytic activity for methyl orange degradation. *Journal of Hazardous Materials*, *155*(3), 572–579.
- Virkutyte, J., Jegatheesan, V., & Varma, R. S. (2012). Visible light activated

TiO_2/microcrystalline cellulose nanocatalyst to destroy organic contaminants in water. *Bioresource Technology*, *113*, 288–293.

- Yagub, M. T., Sen, T. K., Afroze, S., & Ang, H. M. (2014). Dye and its removal from aqueous solution by adsorption: a review. *Advances in Colloid and Interface Science*, *209*, 172–184.
- Zaleska, A. (2008). Doped-TiO_2: a review. *Recent Patents on Engineering*, *2*(3), 157–164.

MSc Dissertation

ORIGINALITY REPORT

6%	3%	4%	%
SIMILARITY INDEX	INTERNET SOURCES	PUBLICATIONS	STUDENT PAPERS

PRIMARY SOURCES

1	iopscience.iop.org Internet Source	<1%
2	Molly Thomas, Gowhar Ahmad Naikoo, Mehraj Ud Din Sheikh, Mustri Bano, Farid Khan. "Effective photocatalytic degradation of Congo red dye using alginate/carboxymethyl cellulose/TiO2 nanocomposite hydrogel under direct sunlight irradiation", Journal of Photochemistry and Photobiology A: Chemistry, 2016 Publication	<1%
3	ecommons.usask.ca Internet Source	<1%
4	Hashem Ahmadizadegan, Sheida Esmaielzadeh, Mahdi Ranjbar, Zahra Marzban, Fatemeh Ghavas. "Synthesis and characterization of polyester bionanocomposite membrane with ultrasonic irradiation process for gas permeation and antibacterial activity", Ultrasonics Sonochemistry, 2018 Publication	<1%

5	Ayodele Temidayo Odularu. "Metal Nanoparticles: Thermal Decomposition, Biomedicinal Applications to Cancer Treatment, and Future Perspectives", Bioinorganic Chemistry and Applications, 2018 Publication	<1%
6	eproceedings.chemistry.utm.my Internet Source	<1%
7	paduaresearch.cab.unipd.it Internet Source	<1%
8	Kazutaka Obata, Kensuke Kishishita, Atsushi Okemoto, Keita Taniya, Yuichi Ichihashi, Satoru Nishiyama. "Photocatalytic decomposition of NH3 over TiO2 catalysts doped with Fe", Applied Catalysis B: Environmental, 2014 Publication	<1%
9	Fan, J.. "Photocatalytic degradation of azo dye by novel Bi-based photocatalyst Bi"4TaO"8I under visible-light irradiation", Chemical Engineering Journal, 20120101 Publication	<1%
10	eprints.kfupm.edu.sa Internet Source	<1%
11	www.chemweb.com Internet Source	<1%

12	Yuanyuan Ma, Qiaofeng Han, Xin Wang, Junwu Zhu. "An in situ annealing route to [Bi6O6(OH)2](NO3)4·2H2O/g-C3N4 heterojunction and its visible-light-driven photocatalytic performance", Materials Research Bulletin, 2018 Publication	<1%
13	facc.co.in Internet Source	<1%
14	Mall, I.D.. "Characterization and utilization of mesoporous fertilizer plant waste carbon for adsorptive removal of dyes from aqueous solution", Colloids and Surfaces A: Physicochemical and Engineering Aspects, 20060420 Publication	<1%
15	Kottakki Naveen Kumar, Karteek Rao Amperayani, V. Ravi Sankar Ummdi, Uma Devi Parimi. "Synthesis and Antimicrobial Activity of Piperine Analogues Containing 1,2,4-Triazole Ring", Asian Journal of Chemistry, 2019 Publication	<1%
16	opus4.kobv.de Internet Source	<1%
17	www.cogentoa.com Internet Source	<1%

18	N. L. Sonar, V. Pardeshi, R. Shukla, M. S. Sonavane, T. P. Valsala, Y. Kulkarni, A. K. Tyagi, C. P. Kaushik, V. K. Manchanda. " Evaluation of Nickel Sulphide Prepared by Different Routes for Removal of Ru from Alkaline Radioactive Liquid Waste ", Separation Science and Technology, 2010 Publication	<1%
19	biochem-molbio.imedpub.com Internet Source	<1%
20	nanobe.org Internet Source	<1%
21	Sharma, A.. "Azadirachta indica (Neem) leaf powder as a biosorbent for removal of Cd(II) from aqueous medium", Journal of Hazardous Materials, 20051017 Publication	<1%
22	B. L. Abrams, J. P. Wilcoxon. "Nanosize Semiconductors for Photooxidation", Critical Reviews in Solid State and Materials Sciences, 2005 Publication	<1%
23	www.ijirae.com Internet Source	<1%
24	environmentaljournals.org Internet Source	<1%

25	Yeit Haan Teow, Li Ming Kam, Abdul Wahab Mohammad. "Synthesis of cellulose hydrogel for copper (II) ions adsorption", Journal of Environmental Chemical Engineering, 2018 Publication	<1%
26	openaccess.iyte.edu.tr Internet Source	<1%
27	www.ndsl.kr Internet Source	<1%
28	Jun Xu, Sisi Li, Feng Wang, Zhouxiaoshuang Yang, Hui Liu. "Efficient and Enhanced Adsorption of Methylene Blue on Triethanolamine-Modified Graphene Oxide", Journal of Chemical & Engineering Data, 2019 Publication	<1%
29	Wan-Kuen Jo, Thillai Sivakumar Natarajan. " Facile Synthesis of Novel Redox-Mediator-free Direct Z-Scheme Caln S Marigold-Flower-like/TiO Photocatalysts with Superior Photocatalytic Efficiency ", ACS Applied Materials & Interfaces, 2015 Publication	<1%
30	Amarja P. Naik, Akshay V. Salkar, Mahesh S. Majik, Pranay P. Morajkar. " Enhanced photocatalytic degradation of Amaranth dye on mesoporous anatase TiO : evidence of C–N, NÆN bond cleavage and identification of new	<1%

intermediates ", Photochemical & Photobiological Sciences, 2017
Publication

31	www.worldscientific.com Internet Source	<1%
32	www.civil.iitm.ac.in Internet Source	<1%
33	Z Aksu. "Equilibrium and kinetic modelling of cadmium(II) biosorption by C. vulgaris in a batch system: effect of temperature", Separation and Purification Technology, 2001 Publication	<1%
34	repositorio.unifesp.br Internet Source	<1%
35	Thybo, Pia, Jakob Kristensen, and Lars Hovgaard. "Characterization and Physical Stability of Tolfenamic Acid-PVP K30 Solid Dispersions", Pharmaceutical Development and Technology, 2007. Publication	<1%
36	Qin, Xingzhen, Ang Lu, and Lina Zhang. "Gelation behavior of cellulose in NaOH/urea aqueous system via cross-linking", Cellulose, 2013. Publication	<1%
37	www.ros.hw.ac.uk	